

CALCULATION OF THE DEEP PENETRATION OF
RADIATION BY THE METHOD OF INVARIANT IMBEDDING

by

Donald R. Mathews

Supervisors: Kent F. Hansen
Edward A. Mason

GPO PRICE \$ _____

CFSTI PRICE(S) \$ _____

Hard copy (HC) 4.00

Microfiche (MF) 1.00

653 July 65

Department of Nuclear Engineering
Massachusetts Institute of Technology
Cambridge, Massachusetts

FEBRUARY, 1966

Work Sponsored in Part by
M. I. T. Center for Space Research
under N A S A Grant NsG-496

N66 21662

(ACCESSION NUMBER)	(THRU)
<u>127</u>	<u>1</u>
(PAGES)	(CODE)
<u>CR-171388</u>	<u>22</u>
(NASA CR OR TMX OR AD NUMBER)	(CATEGORY)

CALCULATION OF THE DEEP PENETRATION OF
RADIATION BY THE METHOD OF INVARIANT IMBEDDING

by

DONALD RICHARD MATHEWS

B. S., University of California
(1958)

M. S., University of California
(1959)

SUBMITTED IN PARTIAL FULFILLMENT

OF THE REQUIREMENTS FOR THE

DEGREE OF DOCTOR OF

PHILOSOPHY

at the

MASSACHUSETTS INSTITUTE OF

TECHNOLOGY

June, 1966

Signature of Author
Department of Nuclear Engineering, Feb. 14, 1966

Certified by
K. F. Hansen, Thesis Supervisor

Accepted by
Chairman, Departmental Committee
on Graduate Students

CALCULATION OF THE DEEP PENETRATION OF
RADIATION BY THE METHOD OF INVARIANT IMBEDDING

by

DONALD RICHARD MATHEWS

SUBMITTED TO THE DEPARTMENT OF NUCLEAR ENGINEERING
ON FEBRUARY 14, 1966 IN PARTIAL FULFILLMENT OF THE
REQUIREMENT FOR THE DEGREE OF DOCTOR OF PHILOSOPHY

N 66-21662

The method of invariant imbedding has been applied to energy dependent shielding problems with anisotropic cross sections. The method seems to offer advantages over competing methods when the shield is either very heterogeneous or heterogeneous and very thick. Plane geometry reflection and transmission equations are derived using the method of invariant imbedding and their numerical solution is discussed. A simple exponential approximation is shown to work well for the solution of these equations. Results for several problems, including thick water and thinner iron/polyethylene/iron shields, are given and compared with other methods.

Author

Thesis Supervisors: Kent F. Kansen
Associate Professor of
Nuclear Engineering

Edward A. Mason
Professor of Nuclear
Engineering (Sabbatical
Leave, 1965-66)

ACKNOWLEDGMENTS

The guidance and support of this work by Professors K. F. Hansen and E. A. Mason of the Nuclear Engineering Department at the Massachusetts Institute of Technology is gratefully acknowledged.

This work was supported in part, by the Atomic Energy Commission through its Special Fellowship Program in Nuclear Science and Engineering, and in part, by the National Aeronautics and Space Administration under research grant NsG-496.

The computations were performed at the M.I.T. Computation Center.

Professor H. Goldstein of Columbia University kindly supplied some of the nuclear cross section data.

TABLE OF CONTENTS

	PAGE
TITLE PAGE	1
ABSTRACT	2
ACKNOWLEDGMENTS	3
TABLE OF CONTENTS	4
LIST OF TABLES	6
LIST OF FIGURES	7
Chapter I. INTRODUCTION	
The Method of Invariant Imbedding	8
Outline of Thesis	12
Chapter II. REFLECTION AND TRANSMISSION IN PLANE GEOMETRY	
Introduction	14
Derivation of Reflection and Transmission Equations	14
Analytic Solution in a Restricted Case	29
Discussion	32
Chapter III. NUMERICAL SOLUTION OF THE REFLECTION AND TRANSMISSION EQUATIONS	
Introduction	33
Reduction to a Finite Set of Differential Equations	33
Solution by Means of Ordinary Methods	38
Solution by Means of Exponential Approximations	39
Discussion	49
Chapter IV. RESULTS	
Introduction	50
Monoenergetic Particles in a Thin Rod	51
Monoenergetic Particles in an Isotropically Scattering Medium	56
Polyenergetic Neutrons in Water	63

	PAGE
Polyenergetic Neutrons in a Heterogeneous Iron/Polyethylene/	
Iron Shield	71
Discussion	74
Chapter V. CONCLUSIONS AND SUGGESTIONS FOR FURTHER WORK	79
APPENDIX A. INPUT DATA PREPARATION	
Introduction	85
Abscissas and Weights for Numerical Integrations	86
Total Cross Section	87
Mean Number of Secondaries per Collision	87
State-to-State Transfer Probability	88
Discussion	94
APPENDIX B. OUTPUT DATA PROCESSING	
Introduction	96
Relations between Reflection and Transmission and other Variables commonly used in Neutron Transport Theory	97
Relation between Point and Plane Sources	100
APPENDIX C. COMPUTER PROGRAM FOR THE SOLUTION OF THE REFLECTION AND TRANSMISSION EQUATIONS	101
APPENDIX D. COMPUTER PROGRAM FOR THE PREPARATION OF INPUT DATA . . .	138
REFERENCES	168
BIOGRAPHICAL SKETCH	172

LIST OF TABLES

TABLE	PAGE
I. Reflection Values for Rod Model With Isotropic Scatter and $C = 0.9$	53
II. Transmission Values for Rod Model With Isotropic Scatter and $C = 0.9$	55
III. Effect of Changes in C and the Error Criterion (three angular groups used)	62
IV. Neutron Dose Transmission Factors for a Unit Isotropic Fission Source Incident Upon Iron/Polyethylene Shields	72
V. Computing Time Required by Invariant Imbedding Problems	75

LIST OF FIGURES

FIGURE		PAGE
1.	Coordinate System	16
2.	Plane Geometry Directions	21
3.	Reflection Versus Rod Length	52
4.	Transmission Versus Rod Length	54
5.	Net Transmitted Flux Versus Number of Angular Groups and Incident Direction	58
6.	Transmitted Current Due to a Unit Isotropic Source Versus the Number of Angular Groups	59
7.	Transmitted Current Due to a Unit Isotropic Source Versus the Error Criterion	61
8.	Dose Rate Due to a Plane Isotropic Fission Neutron Source Versus Water Shield Thickness	65
9.	Dose Rate Versus Distance From a Point Isotropic Fission Neutron Source in Water	67
10.	Neutron Dose Rate in Water Versus Distance From a Point Isotropic Fission Neutron Source	68
11.	Neutron Flux Versus Energy and Distance From a Point Isotropic Fission Source in Water	70
12.	Neutron Dose Transmission Factor for a Unit Isotropic Fission Source Incident upon Iron/Polyethylene Shields .	73
13.	Step Size Variation in the Five Energy Group Problem IV . .	76

CHAPTER I

INTRODUCTION

The Method of Invariant Imbedding

This thesis is concerned with the practical application of a particular formulation of neutral particle transport theory called the method of invariant imbedding to neutron penetration problems.

The invariant imbedding method apparently began with the work of the Russian astrophysicist, Ambarzumian, on the reflection of light from an infinite half space [1] . The formulation of a complete set of "principles of invariance" and their systematic integration into a general theory including finite media, was carried out by Chandrasekhar [2] . The method was applied to neutron transport problems by Bellman, Kalaba, and Wing [3] under the name "invariant imbedding" which seems to have become the accepted name for the method. Invariant imbedding was first applied to neutron shielding problems by Beissner [4] .

Invariant imbedding is not a method for obtaining analytic or numerical solutions of the Boltzmann equation. It is a different approach to the derivation of particle transport equations. The invariant imbedding method concentrates on the radiation flux crossing the boundaries of a region and on how this radiation flux varies as the thickness of the region changes, in contrast to the Boltzmann type formulation in which attention is concentrated on the variation of the radiation density with position inside a region of fixed thickness. The invariant imbedding approach leads to a nonlinear initial value

problem instead of the linear boundary value problem obtained by the Boltzmann approach.

Advantages of the invariant imbedding method for shielding purposes include: 1) results may be obtained over the whole range of possible shield thicknesses in one problem; 2) the results are in a directly useful form, i.e., reflection and transmission matrices which may be used to obtain the reflected and transmitted fluxes for any incident flux; 3) the method applies rigorously to heterogeneous shields without increase in computer memory requirements because of the heterogeneity; 4) the method is efficient for thick shields (deep penetrations) because the time required increases linearly (or less) with the shield thickness, i.e., a 30 mean free path (mfp) thickness requires not more than twice as long as a 15 mfp thickness for the same degree of heterogeneity; and 5) the error in the numerical solution of the discrete approximations to the rigorous invariant imbedding equations may be easily estimated and controlled.

Disadvantages include: 1) the method is fairly time consuming during the initial transient at the beginning of a problem and does not appear to be economically competitive with other methods such as the Monte Carlo method when the shield is thin and 2) the method is not easy to apply in other than plane geometry, hence only the plane geometry problem is considered in this thesis although the invariant imbedding method has been used to derive neutral particle transport equations in spherical and cylindrical geometries by Bellman, Kalaba, and Wing [5, 21] .

The derivation of plane geometry reflection and transmission

equations by the invariant imbedding method given in Chapter II follows the work of Chandrasekhar in that the transmission equation is written in terms of the diffuse transmission rather than the total transmission used by Bellman, Kalaba, and Wing. It was pointed out by Beissner [6] that there is both theoretical and experimental justification for performing separate calculations for the uncollided flux and the diffuse (scattered) flux. The angular distribution of the total transmission is very anisotropic at small thicknesses because of the delta function initial condition whereas the angular distribution of the diffuse transmission is relatively smooth in the region, leading one to suspect that a lower order angular approximation may suffice for accurate calculation of the diffuse transmission than for the total transmission.

No restriction on the position or energy dependence of the cross sections other than the one dimensional character of the plane geometry problem are made in the basic derivation, although the numerical solution is restricted to media composed of discrete layers. The number of discrete layers may be as large as desired and this is one of the very real advantages of the method. Because of the initial value character of the problem, the solution starts at zero thickness and builds up a slab shield one layer at a time so that, in principle, different cross sections could be used for each layer.

The scattering process is restricted to the azimuthally symmetric case since this is the case of practical interest. This assumption means that the scattering process is assumed to depend only upon the initial and final energies and the angle of deflection. This restriction is not necessary and a reflection equation for the general case is given

in Chapter II.

The boundary conditions are exact in the sense that they are inherent in the problem formulation and are satisfied exactly in all orders of approximation in contrast to methods such as the spherical harmonics (P_n) method in which the boundary conditions are only satisfied approximately.

The results of this work indicate that the most useful applications of the invariant imbedding method in plane geometry will probably be to problems in which the moments method does not apply because of heterogeneity and, in which the attenuation is large enough to make the Monte Carlo method unattractive on account of excessive computing time and, in which the scattering is sufficiently anisotropic to make the application of the usual varieties of SNG or DSN type transport theory solutions suspect.

The transmission matrix method of Yarmush, Zell, and Aronson [28] which also uses reflection and transmission matrices can be regarded as a special technique for obtaining numerical solutions of the Boltzmann type boundary value problem. This method requires the diagonalization and inversion of matrices containing the material properties for each homogeneous layer of a shield and the subsequent combination of this information into an overall transfer matrix for the shield containing both the reflection and transmission matrices and is quite different from the invariant imbedding method in which integration of a coupled set of differential equations subject to specified initial conditions replaces the matrix inversions at each thickness of each layer. Both methods may be used to generate reflection and transmission matrices

that may be tabulated for future use.

The original impetus to investigate the application of the invariant imbedding method to neutron shielding problems was provided by the work of Beissner [4] . It appears that the later work by Beissner [6] on the penetration of neutrons through thin homogeneous polyethylene slabs is the only other application of the invariant imbedding method to energy dependent problems reported to date. It is hoped that this thesis has added sufficiently to the development and practical application of the invariant imbedding method so that other investigators will also be encouraged to try the method.

Outline of Thesis

In Chapter II the invariant imbedding method is used to derive rigorous equations for the reflection and transmission of neutral particles in plane geometry. An analytic solution of the reflection and transmission equations in a very restricted case is also presented.

The numerical solution of these reflection and transmission equations is discussed in Chapter III. First, the rigorous equations are approximated by a finite set of coupled first-order nonlinear differential equations subject to specified initial conditions. Various numerical techniques for the solution of this set of differential equations are discussed and exponential approximations are introduced in order to take advantage of the physics of the radiation penetration problem. The application of the simplest and most successful of the exponential approximations to the solution of the reflection and transmission equations is presented along with the results of an

investigation of the stability of the approximation.

Numerical results for four different problems are presented in Chapter IV. The first two problems are restricted to the monoenergetic (one velocity) case and are presented to show some aspects of the characteristic behavior of the reflection and transmission variables and to verify the numerical solution technique before proceeding to more complicated cases. The third problem considers the penetration of neutrons through large thicknesses of water (up to 210 cm). Satisfactory agreement between the invariant imbedding results and other transport theory methods is shown for both the transmitted neutron dose rate and for the neutron energy spectrum. The fourth problem considers a relatively thin three layer iron-polyethylene-iron shield. Satisfactory agreement between Monte Carlo method results for this shield and the invariant imbedding results is shown.

Conclusions and suggestions for further work are discussed in Chapter V.

The details of the input and output data processing and the associated computer codes are presented in the appendices.

While it is clear that some items are relatively more important than others, the reader is cautioned that in computer oriented work such as this, there are no truly unimportant details. The deep penetration problem is very sensitive to small details because of the very great attenuation. An attempt has been made to point out the most serious difficulties encountered in this work.

CHAPTER II

REFLECTION AND TRANSMISSION IN PLANE GEOMETRY

Introduction

Equations for the reflection and transmission of radiation by a slab of finite thickness in one dimension and of infinite extent in the other two dimensions are derived in this chapter by means of the method of invariant imbedding. No restrictions on the position or energy dependence of the cross sections are made other than the one dimensional character of the problem.

The reflection and transmission equations (2.31) and (2.32) are specialized to the case of practical interest in which the scattering process is assumed to be azimuthally symmetric, i.e., that the scattering process depends only upon the initial and final energies and the angle of deflection. This restriction is not necessary and the reflection equation for the general case is given in equation (2.24).

The boundary conditions are exact in the sense that they are inherent in the problem formulation and are satisfied exactly in all orders of approximation. The practical case with azimuthally symmetric scattering considers a monoenergetic conical source of strength $1/2\pi$ per unit time with energy E^0 and direction cosine μ^0 (see Fig. 2).

The analytic solution of these reflection and transmission equations is given for the monoenergetic case with scattering in only the z direction in a homogeneous medium.

Derivation of Reflection and Transmission Equations

Consider a slab extending from $z=0$ to $z=s$ and of infinite extent in the x and y directions. Let \vec{r} be a position vector from the origin

of the x, y, z coordinate system to the particle position. Let the particle direction be specified by the unit vector \hat{n} where \hat{n} is specified by the polar angle θ and the azimuthal angle ϕ as shown in Fig. 1. The unit vector \hat{n} has components

$$\begin{aligned}\hat{n}_x &= \sin \theta \cos \phi \\ \hat{n}_y &= \sin \theta \sin \phi \\ \hat{n}_z &= \cos \theta\end{aligned}\tag{2.1}$$

The element of solid angle $d\Omega$ around \hat{n} is

$$d\Omega = \sin \theta \, d\theta \, d\phi .\tag{2.2}$$

Defining

$$\cos \theta = \mu\tag{2.3}$$

then

$$d\Omega = d\mu \, d\phi .\tag{2.4}$$

The position vector r has components

$$\begin{aligned}x &= r \sin \theta \cos \phi \\ y &= r \sin \theta \sin \phi \\ z &= r \cos \theta\end{aligned}\tag{2.5}$$

The differential element of volume dV around r is

$$\begin{aligned}dV &= dr \, r^2 \sin \theta \, d\theta \, d\phi \, dr \\ &= r^2 \, d\Omega \, dr \\ &= r^2 \, d\mu \, d\phi \, dr .\end{aligned}\tag{2.6}$$

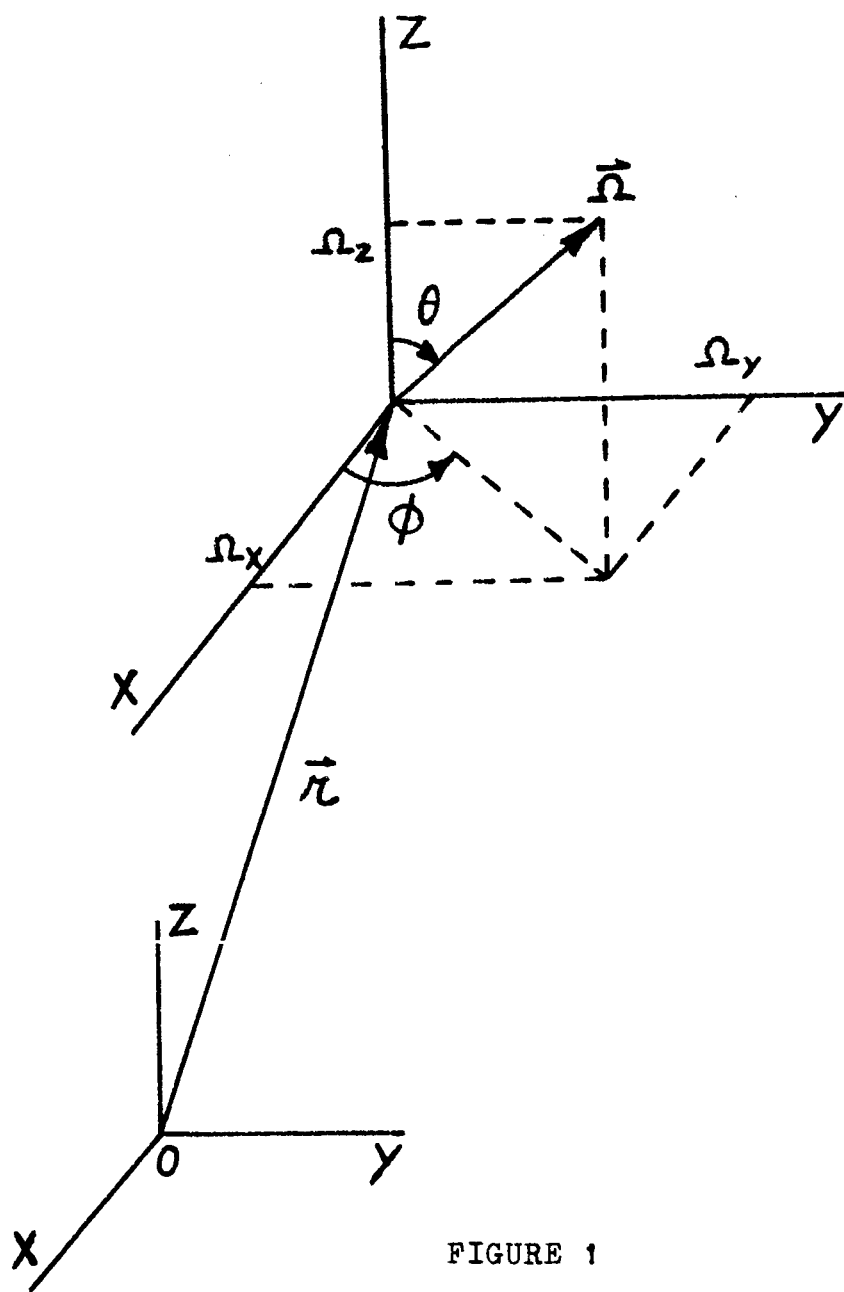


FIGURE 1

COORDINATE SYSTEM

Let $N(\vec{r}, \vec{\Omega}, E, t) dV d\Omega dE$ represent the number of particles whose position vectors lie within dV around \vec{r} , whose directions lie within $d\Omega$ around $\vec{\Omega}$, whose energies lie within dE around E , measured at time t . Then the number of particles, per unit volume at position \vec{r} , per unit energy at energy E , at time t , is

$$n(r, E, t) = \int N(r, \vec{\Omega}, E, t) d\Omega \quad (2.7)$$

Let the vector velocity be \vec{v} and the scalar velocity be v .

Then

$$\vec{v} = v\vec{\Omega}. \quad (2.8)$$

The number of particles per unit time, passing through a unit area normal to the direction of motion $\vec{\Omega}$, at position \vec{r} , per unit energy E , at time t , is $vN(\vec{r}, \vec{\Omega}, E, t)$. The number of particles per unit time, passing through a unit area in the x, y plane, at position \vec{r} , per unit energy at energy E , at time t , is $|\cos\theta| vN(\vec{r}, \vec{\Omega}, E, t)$.

$N(\vec{r}, \vec{\Omega}, E, t)$ and $vN(\vec{r}, \vec{\Omega}, E, t)$ will be called the "angular density" and the "angular flux" respectively.

The number of particles interacting per unit time, per unit volume at position \vec{r} , per unit solid angle in direction $\vec{\Omega}$, per unit energy at energy E , at time t , is $\sigma(\vec{r}, E, t) vN(\vec{r}, \vec{\Omega}, E, t)$ where

$\sigma(\vec{r}, E, t)$ is the total macroscopic cross section (units of inverse distance).

The quantity $[\sigma(\vec{r}, E, t) d]$ represents (to first order in d the probability that a particle will undergo an interaction in passing through a distance d . In passing from z to $z + h$, a particle travels a distance

$$d = h / |\cos\theta|. \quad (2.9)$$

Now consider only time independent cases and suppress the time variable. Let $f(\vec{r}, \vec{\Omega}, E; \vec{\Omega}', E') dE d\Omega$ be the probability that a particle with initial energy E' and direction of motion $\vec{\Omega}'$, will emerge after an interaction with a target nucleus with an energy in dE about E and a direction of motion in $d\Omega$ about $\vec{\Omega}$. The quantity $f(\vec{r}, \vec{\Omega}, E; \vec{\Omega}', E')$ is normalized so that the integral over all exit energies and exit directions is unity, i.e.,

$$\int dE \int d\Omega f(\vec{r}, \vec{\Omega}, E; \vec{\Omega}', E') = 1 \quad (2.10)$$

In the case of azimuthally symmetric interactions with stationary nuclei, the usual case, the probability that a particle will emerge in any particular direction can only depend on (at most) the particle's initial and final energies and on the angle between its original direction $\vec{\Omega}'(\theta', \phi')$ and its direction after collision $\vec{\Omega}(\theta, \phi)$. Let

$$\cos \theta_0 = \mu_0 = \vec{\Omega} \cdot \vec{\Omega}' \quad (2.11)$$

Then

$$\mu_0 = \mu \mu' + \sqrt{1-\mu^2} \sqrt{1-(\mu')^2} \cos(\phi - \phi') \quad (2.12)$$

and we can now define a quantity $g(\vec{r}, \mu, E; \mu', E')$ such that

$$g(\vec{r}, \mu, E; \mu', E') dE d\mu = \int_0^{2\pi} d\phi' f(\vec{r}, \vec{\Omega}, E; \vec{\Omega}', E') dE d\Omega \quad (2.13)$$

is the probability that a particle with initial energy E' and initial direction cosine μ' will emerge after a collision with an energy in dE about E and a direction cosine in $d\mu$ about μ .

Let $C(\vec{r}, E')$ be the mean number of secondaries per collision

where

$$C(\vec{r}, E') = \left[\nu(\vec{r}, E') \sigma_f(\vec{r}, E') + \sigma_e(\vec{r}, E') + \sigma_{in}(\vec{r}, E') + 2 \sigma_{n2n}(\vec{r}, E') \right] / \sigma(\vec{r}, E') \quad (2.14)$$

and where σ_f , σ_e , σ_{in} , σ_{n2n} , and σ are the fission, inelastic, elastic, n,2n, and total cross sections, respectively and ν is the mean number of neutrons per fission.

The total expected number of particles per unit time, per unit volume at position \vec{r} , transferred into dE about E and into $d\Omega$ about $\vec{\Omega}$ from all other energies and directions is

$$\begin{aligned} dEd\Omega \int dE' \int d\Omega' \nu' N(\vec{r}, \Omega', E') \sigma(\vec{r}, E') C(\vec{r}, E') f(\vec{r}, \vec{\Omega}, E; \vec{\Omega}', E') \\ = N(\vec{r}, \vec{\Omega}, E) dEd\Omega \end{aligned} \quad (2.15)$$

Now let there be incident upon the $z=s$ face of the slab an angular flux of one particle per unit time, per unit area normal to the direction of motion, with energy E' and direction $\vec{\Omega}'$. For this flux, (2.15) becomes

$$\left(\int dE'' \int d\Omega'' \delta(\Omega'' - \Omega') \delta(E'' - E') \sigma(\vec{r}, E'') f(\vec{r}, \vec{\Omega}, E; \vec{\Omega}'', E'') \right) C(\vec{r}, E') = \sigma(\vec{r}, E') C(\vec{r}, E') f(\vec{r}, \vec{\Omega}, E; \vec{\Omega}', E') \quad (2.16)$$

where the differentials $dEd\Omega$ have been cancelled out.

For this input define an angular reflected flux $r(s, \vec{\Omega}, E; \vec{\Omega}', E') dEd\Omega$ representing the expected number of particles per unit time reflected through a unit area normal to the direction of motion, at position $z=s$, with energy in dE about E and direction in $d\Omega$ about $\vec{\Omega}$.

Now add an additional layer of thickness h to the $z=s$ face of

the slab and account for the particles reflected from the slab of thickness $s+h$ in terms of the reflection from the slab of thickness s plus interactions in the layer of thickness h (see Fig. 2). The slab properties are assumed to be uniform in the x,y plane and variable with position in the z direction. The distance travelled by an incident particle in traversing the layer of thickness h is

$$d = h / |\mu'| \quad (2.17)$$

where $-1 \leq \mu' < 0$.

The probability that an incident particle will interact while traversing the layer of thickness h is (to first order in h)

$$\sigma(s, E') h / |\mu'| \quad (2.18)$$

The reflected angular flux due to interactions of the incident angular flux with the material of the layer of thickness h is (to first order in h)

$$\sigma(s, E')(h / |\mu'|) C(s, E') f(s, \mu, \varphi, E; \mu', \varphi', E') \quad (2.19)$$

where $-1 \leq \mu' < 0$, $0 \leq \mu < 1$, $0 \leq \varphi' \leq 2\pi$, and $0 \leq \varphi \leq 2\pi$.

The angular flux incident upon the $z=s$ face of the slab due to interactions of the incident angular flux with the material of the layer of thickness h is (to first order in h)

$$\sigma(s, E')(h / |\mu'|) C(s, E') f(s, \mu, \varphi, E; \mu', \varphi', E') \quad (2.20)$$

where $-1 \leq \mu' < 0$, $-1 \leq \mu < 0$, $0 \leq \varphi' \leq 2\pi$, and $0 \leq \varphi \leq 2\pi$.

The probability that an incident particle can pass from $z=s$ to $z=s+h$ without interaction is given by (to first order in h)

$$1 - \sigma(s, E')(h / |\mu'|) \quad (2.21)$$

where $-1 \leq \mu' < 0$.

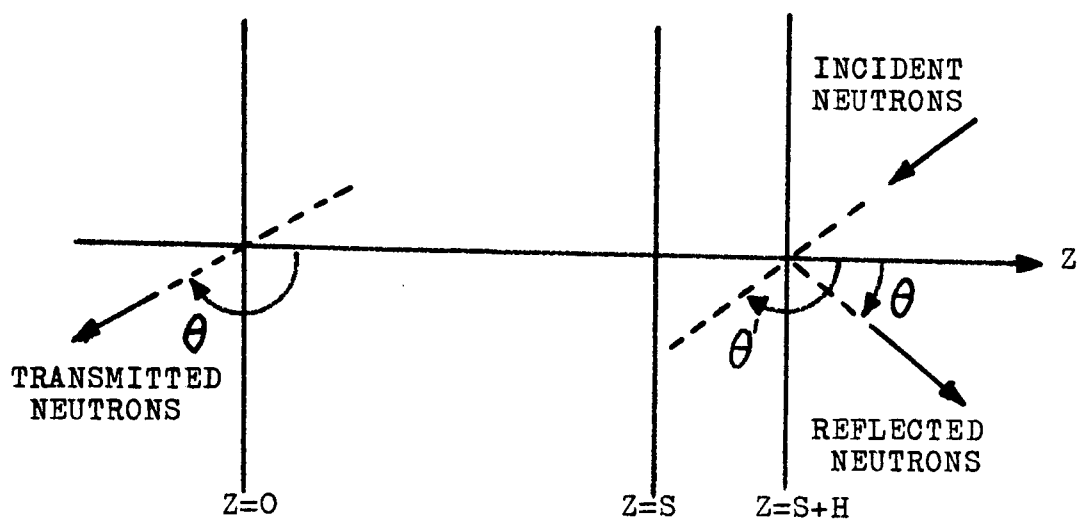


FIGURE 2

PLANE GEOMETRY DIRECTIONS

Now sum up all processes leading to terms of first order or less in h to obtain

$$\begin{aligned}
 r(s+h, \mu, \phi, E; \mu', \phi', E') = & \\
 & \sigma(s, E')(h/|\mu'|)C(s, E')f(s, \mu, \phi, E; \mu', \phi', E') + \\
 & \left(\int_{-1}^0 d\mu'' \int_0^{2\pi} d\phi'' \int_0^\infty dE'' \sigma(s, E')(h/|\mu''|)C(s, E') \right. \\
 & \quad \left. f(s, \mu'', \phi'', E''; \mu', \phi', E') r(s, \mu, \phi, E; \mu'', \phi'', E'') \right. \\
 & \quad \left. [1 - \sigma(s, E)(h/\mu)] \right) + \left([1 - \sigma(s, E')(h/|\mu'|)] \right. \\
 & \quad \left. r(s, \mu, \phi, E; \mu', \phi', E') [1 - \sigma(s, E)(h/\mu)] \right) + \left(\int_0^1 d\mu'' \right. \\
 & \quad \left. \int_0^{2\pi} d\phi'' \int_0^\infty dE'' [1 - \sigma(s, E')(h/|\mu''|)] r(s, \mu'', \phi'', E''; \mu', \phi', E') \right. \\
 & \quad \left. \sigma(s, E'')(h/\mu'')C(s, E'')f(s, \mu, \phi, E; \mu'', \phi'', E'') \right) + \left(\int_0^1 d\mu'' \right. \\
 & \quad \left. \int_0^\infty d\mu'' \int_0^{2\pi} d\phi'' \int_0^{2\pi} d\phi'' \int_0^\infty dE'' \int_0^\infty dE'' [1 - \sigma(s, E')(h/|\mu'|)] \right. \\
 & \quad \left. r(s, \mu'', \phi'', E''; \mu', \phi', E') \sigma(s, E'')(h/\mu'')C(s, E'') \right. \\
 & \quad \left. f(s, \mu'', \phi'', E''; \mu'', \phi'', E'') r(s, \mu, \phi, E; \mu'', \phi'', E'') \right. \\
 & \quad \left. [1 - \sigma(s, E)(h/\mu)] \right) + O(h^2) \tag{2.22}
 \end{aligned}$$

where $-1 \leq \mu' < 0$, $0 < \mu \leq 1$, $0 \leq \phi' \leq 2\pi$, and $0 \leq \phi \leq 2\pi$.

The various terms on the right hand side of (2.22) may be explained as follows: the first term is (to order h) the probability that a particle will interact in $(s+h, s)$ and be back scattered; the second term is the probability that a particle will interact in $(s+h, s)$ and be forward scattered times the probability of reflection from the $z=s$ face

times the probability of no interaction in $(s, s+h)$; the third term is the probability of no interaction in $(s+h, s)$ times the probability of reflection from the $z=s$ face times the probability of no interaction in $(s, s+h)$; the fourth term is the probability of no interaction in $(s+h, s)$ times the probability of reflection from the $z=s$ face times the probability of interaction in $(s, s+h)$ followed by forward scatter; the fifth term is the probability of no interaction in $(s+h, s)$ times the probability of reflection from the $z=s$ face times the probability of interaction in $(s, s+h)$ followed by backward scatter times the probability of reflection from the $x=s$ face times the probability of no interaction in $(s, s+h)$; and the last term represents terms of order h^2 and higher.

Equation (2.22) may be rewritten in the following form

$$\begin{aligned}
 & \frac{r(s+h, \mu, \phi, E; \mu', \phi', E') - r(s, \mu, \phi, E; \mu', \phi', E')}{h} = \\
 & \sigma(s, E')(1/|\mu'|)C(s, E')f(s, \mu, \phi, E; \mu', \phi', E') + \\
 & \left(\int_{-1}^0 d\mu'' \int_{-1}^0 d\phi'' \int_0^\infty dE'' \frac{\sigma(s, E')}{|\mu'|} C(s, E')f(s, \mu'', \phi'', E''; \mu', \phi', E') \right. \\
 & \quad \left. r(s, \mu, \phi, E; \mu'', \phi'', E'') - \left[\frac{\sigma(s, E')}{|\mu'|} + \frac{\sigma(s, E)}{\mu} \right] \right. \\
 & \quad \left. r(s, \mu, \phi, E; \mu', \phi', E') \right) + \left(\int_0^1 d\mu'' \int_0^{2\pi} d\phi'' \int_0^\infty dE'' \right. \\
 & \quad \left. r(s, \mu'', \phi'', E''; \mu', \phi', E') \frac{\sigma(s, E'')}{\mu''} C(s, E'')f(s, \mu, \phi, E; \mu'', \phi'', E'') \right) + \\
 & \left(\int_0^1 d\mu'' \int_{-1}^0 d\mu'' \int_0^{2\pi} d\phi'' \int_0^{2\pi} d\phi'' \int_0^\infty dE'' \int_0^\infty dE'' \right. \\
 & \quad \left. r(s, \mu'', \phi'', E''; \mu', \phi', E') \frac{\sigma(s, E'')}{\mu''} C(s, E'') \right. \\
 & \quad \left. f(s, \mu'', \phi'', E''; \mu'', \phi'', E'') r(s, \mu, \phi, E; \mu'', \phi'', E'') \right) + \\
 & O(h) \quad (2.23)
 \end{aligned}$$

Now take the limit as h approaches zero to obtain a general equation for the reflection in plane geometry in the form

$$\begin{aligned}
 \frac{d}{ds} r(s, \mu, \varphi, E; \mu', \varphi', E') = & \\
 & \frac{\sigma(s, E')}{|\mu'|} C(s, E') f(s, \mu, \varphi, E; \mu', \varphi', E') + \\
 & \left(\int_0^1 d\mu'' \int_0^{2\pi} d\varphi'' \int_0^\infty dE'' \frac{\sigma(s, E')}{|\mu'|} C(s, E') f(s, \mu'', \varphi'', E''; \mu', \varphi', E') \right. \\
 & \left. r(s, \mu, \varphi, E; \mu'', \varphi'', E'') \right) - \left(\left[\frac{\sigma(s, E')}{|\mu'|} + \frac{\sigma(s, E)}{\mu} \right] \right. \\
 & \left. r(s, \mu, \varphi, E; \mu', \varphi', E') \right) + \left(\int_0^1 d\mu'' \int_0^{2\pi} d\varphi'' \int_0^\infty dE'' \right. \\
 & \left. r(s, \mu'', \varphi'', E''; \mu', \varphi', E') \frac{\sigma(s, E'')}{|\mu''|} C(s, E'') f(s, \mu, \varphi, E; \mu'', \varphi'', E'') \right) + \\
 & \int_0^1 d\mu'' \int_0^{2\pi} d\varphi'' \int_0^\infty dE'' \int_0^\infty dE''' r(s, \mu'', \varphi'', E''; \mu', \varphi', E') \\
 & \frac{\sigma(s, E''')}{|\mu''|} C(s, E''') f(s, \mu'', \varphi'', E''; \mu'', \varphi'', E'') \\
 & r(s, \mu, \varphi, E; \mu''', \varphi''', E''') \quad (2.24)
 \end{aligned}$$

When the scattering is azimuthally symmetric, the reflection is not a function of the azimuthal angle and

$$\int_0^{2\pi} d\varphi r(s, \mu, \varphi, E; \mu', \varphi', E') = 2\pi r(s, \mu, E; \mu', E'). \quad (2.25)$$

Using (2.13) and (2.25) in (2.24) yields

$$\begin{aligned}
\frac{d}{ds} r(s, \mu, E; \mu', E') = & \\
\frac{1}{2\pi} \frac{\sigma(s, E')}{|\mu'|} C(s, E') g(s, \mu, E; \mu', E') + & \\
\int_{-1}^0 d\mu'' \int_0^\infty dE'' \frac{\sigma(s, E')}{|\mu'|} C(s, E') g(s, \mu'', E''; \mu', E') r(s, \mu, E; \mu'', E'') - & \\
\left[\frac{\sigma(s, E')}{|\mu'|} + \frac{\sigma(s, E)}{\mu} \right] r(s, \mu, E; \mu', E') + & \\
\int_0^1 d\mu'' \int_0^\infty dE'' r(s, \mu'', E''; \mu', E') \frac{\sigma(s, E'')}{\mu''} C(s, E'') g(s, \mu, E; \mu'', E'') + & \\
2\pi \left(\int_0^1 d\mu'' \int_{-1}^0 d\mu''' \int_0^\infty dE'' \int_0^\infty dE''' r(s, \mu''', E'''; \mu', E') \frac{\sigma(s, E'')}{\mu''} C(s, E'') \right. & \\
\left. g(s, \mu''', E'''; \mu'', E'') r(s, \mu, E; \mu'', E'') \right) & \quad (2.26)
\end{aligned}$$

where $-1 \leq \mu' < 0$, $0 \leq \mu \leq 1$ and the initial condition is

$$r(0, \mu, E; \mu', E') = 0 \quad (2.27)$$

The equation for the diffuse transmission analogous to equation (2.22)

is,

$$\begin{aligned}
t(s+h, \mu, \varphi, E; \mu', \varphi', E') = & \\
\left(\sigma(s, E') (h/|\mu'|) C(s, E') f(s, \mu, \varphi, E; \mu', \varphi', E') \right. & \\
\left. \exp \left[-(1/|\mu|) \int_s^s \sigma(s', E) ds' \right] \right) + & \\
\left(\int_{-1}^0 d\mu'' \int_0^{2\pi} d\varphi'' \int_0^\infty dE'' \sigma(s, E') \frac{h}{|\mu'|} C(s, E') \right. & \\
\left. f(s, \mu'', \varphi'', E''; \mu', \varphi', E') t(s, \mu, \varphi, E; \mu'', \varphi'', E'') \right) + & \\
\left[1 - \sigma(s, E') \frac{h}{|\mu'|} \right] t(s, \mu, \varphi, E; \mu', \varphi', E') + &
\end{aligned}$$

$$\begin{aligned}
& \left(\int_0^1 d\mu'' \int_0^{2\pi} d\phi'' \int_0^\infty dE'' \left[1 - \sigma(s, E') \frac{h}{|\mu'|} \right] r(s, \mu'', \phi'', E''; \mu', \phi', E') \right. \\
& \quad \frac{\sigma(s, E'')}{\mu''} h C(s, E'') f(s, \mu, \phi, E; \mu'', \phi'', E'') \exp \left[-(1/\mu) \right. \\
& \quad \left. \int_0^s \sigma(s', E) ds' \right] \Bigg) + \left(\int_0^1 d\mu'' \int_{-1}^0 d\mu'' : \int_0^{2\pi} d\phi'' \int_0^{2\pi} d\phi'' : \right. \\
& \quad \left. \int_0^\infty dE'' \int_0^\infty dE'' : \left[1 - \sigma(s, E') \frac{h}{|\mu'|} \right] r(s, \mu'', \phi'', E''; \right. \\
& \quad \left. \mu', \phi', E') h \frac{\sigma(s, E'')}{\mu''} C(s, E'') f(s, \mu''', \phi''', E'''; \mu'', \phi'', E'') \right. \\
& \quad \left. t(s, \mu, \phi, E; \mu''', \phi''', E''') \right) + O(h^2) \quad (2.28)
\end{aligned}$$

where $-1 \leq \mu' < 0$, $-1 \leq \mu < 0$, $0 \leq \phi' \leq 2\pi$, $0 \leq \phi \leq 2\pi$.

The various terms on the right hand side of (2.28) may be explained as follows: the first term is (to order h) the probability that a particle will interact in $(s+h, s)$, be scattered forward, and penetrate the slab of thickness s without further interaction; the second term is the probability that a particle will interact in $(s+h, s)$, be forward scattered, and diffusely transmitted; the third term is the probability of no interaction in $(s+h, s)$ times the probability of diffuse transmission through the remainder of the slab; the fourth term is the probability of no interaction in $(s+h, s)$ times the probability of reflection from the $z=s$ face times the probability of interaction in $(s, s+h)$ followed by backward scatter times the probability of no further interaction; the fifth term is the probability of no interaction in $(s+h, s)$ times the probability of reflection from the $z=s$ face times the probability of interaction $(s, s+h)$ followed by backward scatter times the probability of diffuse transmission through the rest of the

slab; and the last term represents terms of order h^2 or higher.

The diffuse transmission equation for the case with azimuthal symmetry is

$$\begin{aligned}
 \frac{d}{ds} t(s, \mu, E; \mu', E') = & \\
 & \frac{1}{2\pi} \frac{\sigma(s, E')}{|\mu'|} C(s, E') g(s, \mu, E; \mu', E') \exp \left[-(1/|\mu|) \int_0^s \sigma(s', E) ds' \right] + \left(\int_{-1}^0 d\mu'' \int_0^\infty dE'' \frac{\sigma(s, E')}{|\mu'|} C(s, E') \right. \\
 & g(s, \mu'', E''; \mu', E') t(s, \mu, E; \mu'', E'') \Big) - \frac{\sigma(s, E')}{|\mu'|} t(s, \mu, E; \mu', E') + \\
 & \left(\int_0^1 d\mu'' \int_0^\infty dE'' r(s, \mu'', E''; \mu', E') \frac{\sigma(s, E'')}{\mu''} C(s, E'') g(s, \mu, E; \mu'', E'') \right. \\
 & \exp \left[-(1/|\mu|) \int_0^s \sigma(s', E) ds' \right] \Big) + 2\pi \left(\int_0^1 d\mu'' \int_{-1}^0 d\mu''' \int_0^\infty dE'' \int_0^\infty dE''' \right. \\
 & r(s, \mu'', E''; \mu', E') \frac{\sigma(s, E'')}{\mu''} C(s, E'') g(s, \mu''', E'''; \mu'', E'') t(s, \mu, E; \mu''', E''') \Big) \quad (2.29)
 \end{aligned}$$

where $-1 \leq \mu' < 0$, $-1 \leq \mu < 0$, and the initial condition is

$$t(0, \mu, E; \mu', E') = 0 \quad (2.30)$$

The factors of π in (2.26) and (2.29) can be eliminated and these equations transformed into a more symmetric form by making the substitutions $R(s, \mu, E; \mu', E') = r(s, \mu, E; \mu', E') / (4|\mu'|)$ and $T(s, \mu, E; \mu', E') = t(s, \mu, E; \mu', E') / (4|\mu'|)$. This is equivalent to changing the incident flux leading to (2.16) from one particle per unit time, per unit area normal to the direction of motion, with energy E' and direction $\vec{\Omega}'$ to an incident flux of $1/4\pi$ particles per unit time, per unit area in the x, y plane, with energy E' and direction $\vec{\Omega}'$.

With this transformation (2.26) becomes

$$\begin{aligned}
 \frac{d}{ds} R(s, \mu, E; \mu', E') &= 2 \sigma(s, E') C(s, E') g(s, \mu, E; \mu', E') + \\
 &\int_{-1}^0 \frac{d\mu''}{|\mu''|} \int_0^\infty dE'' \sigma(s, E') C(s, E') g(s, \mu'', E''; \mu', E') R(s, \mu, E; \mu'', E'') - \\
 &\left[\frac{\sigma(s, E')}{|\mu'|} + \frac{\sigma(s, E)}{\mu} \right] R(s, \mu, E; \mu', E') + \\
 &\int_0^1 \frac{d\mu''}{\mu''} \int_0^\infty dE'' R(s, \mu'', E''; \mu', E') \sigma(s, E'') C(s, E'') g(s, \mu, E; \mu'', E'') + \\
 &\left(\frac{1}{2} \int_0^1 \frac{d\mu''}{\mu''} \int_0^\infty dE'' \int_{-1}^0 \frac{d\mu'''}{|\mu'''|} \int_0^\infty dE''' R(s, \mu''', E'''; \mu', E') \sigma(s, E''') C(s, E''') \right. \\
 &\left. g(s, \mu''', E'''; \mu'', E'') R(s, \mu, E; \mu''', E''') \right) \quad (2.31)
 \end{aligned}$$

and (2.29) becomes

$$\begin{aligned}
 \frac{d}{ds} T(s, \mu, E; \mu', E') &= \\
 &2 \sigma(s, E') C(s, E'') g(s, \mu, E; \mu', E') \exp \left[- \frac{1}{|\mu|} \int_0^s \sigma(s', E) ds' \right] + \\
 &\int_{-1}^0 \frac{d\mu''}{|\mu''|} \int_0^\infty dE'' \sigma(s, E') C(s, E') g(s, \mu'', E''; \mu', E') T(s, \mu, E; \mu'', E'') - \\
 &\frac{\sigma(s, E')}{|\mu'|} T(s, \mu, E; \mu', E') + \\
 &\left(\int_0^1 \frac{d\mu''}{\mu''} \int_0^\infty dE'' R(s, \mu'', E''; \mu', E') \sigma(s, E'') C(s, E'') g(s, \mu, E; \mu'', E'') \right. \\
 &\left. \exp \left[- \frac{1}{|\mu|} \int_0^s \sigma(s', E) ds' \right] + \right. \\
 &\left. \left(\frac{1}{2} \int_0^1 \frac{d\mu''}{\mu''} \int_0^\infty dE'' \int_{-1}^0 \frac{d\mu'''}{|\mu'''|} \int_0^\infty dE''' R(s, \mu''', E'''; \mu', E') \sigma(s, E''') C(s, E''') \right. \right. \\
 &\left. \left. g(s, \mu''', E'''; \mu'', E'') T(s, \mu, E; \mu''', E''') \right) \right) \quad (2.32)
 \end{aligned}$$

Equations (2.31) and (2.32) are the basic equations for the

energy and angle dependent reflection from the transmission through a slab of thickness s in plane geometry.

The only assumption made in deriving these equations was that the scattering process was assumed to be azimuthally symmetric, i.e., that the scattering process depends only upon the initial and final energies and the angle of deflection.

The boundary conditions are exact for the case in which no particles except those from the source are incident upon either face of the slab. No restrictions on the position or energy dependence of the cross sections were necessary.

Equation (2.24) with the substitution of $R(s, \mu, E; \mu', E') / (4|\mu'|)$ for $r(s, \mu, E; \mu', E')$ is in the monoenergetic case the same as the reflection equation given by Chandrasekhar [2]. The corresponding transmission equation is nearly but not quite the same as the monoenergetic transmission equation given by Chandrasekhar. Chandrasekhar's version is valid only for a homogeneous medium, i.e., the factor $\exp\left[-(1/\mu) \int_0^s \sigma(s', E) ds'\right]$ would be $\exp\left[-(1/\mu)\sigma(s, E) s\right]$ in Chandrasekhar's version.

Analytic Solution in a Restricted Case

Analytic solutions of the reflection and transmission equations may be obtained for very restricted cases. If particles are assumed to 1) travel only in the $\pm z$ direction and 2) not to change energy and 3) if the medium is homogeneous, equations (2.31) and (2.32) reduce to

$$\begin{aligned}
\frac{d}{ds} R(s) &= 2\sigma C g(1,-1) + \sigma C g(-1,-1) R(s) - \\
&\quad 2\sigma R(s) + R(s) \sigma C g(1,1) + \\
&\quad \frac{1}{2} R(s) \sigma C g(1,-1) R(s)
\end{aligned} \tag{2.33}$$

and

$$\begin{aligned}
\frac{d}{ds} T(s) &= 2\sigma C g(-1,-1) \exp(-\sigma s) + \sigma C g(-1,-1) T(s) - \\
&\quad \sigma T(s) + R(s) \sigma C g(-1,1) \exp(-\sigma s) + \\
&\quad \frac{1}{2} R(s) \sigma C g(1,-1) T(s)
\end{aligned} \tag{2.34}$$

where

$$R(0) = T(0) = 0. \tag{2.35}$$

Note that

$$g(-1,-1) = g(1,1) \tag{2.36}$$

and

$$g(1,-1) = g(-1,1) \tag{2.37}$$

because in the first case the particle direction does not change and in the second case the direction change is the same (180 degrees).

Equation (2.33) for the reflection can be solved directly by the standard technique for a first order differential equation of the Ricatti type [7]. The result is

$$R(s) = \frac{2}{\sqrt{A^2 - 1} \coth(Bs) - A} \quad (2.38)$$

where

$$A = \frac{C g(1,1)}{C g(1,-1)} - 1 \quad (2.39)$$

and

$$B = \sigma C g(1,-1) \sqrt{A^2 - 1} \quad (2.40)$$

Equation (2.38) for the reflection is the same as given by Wing [8] .

Equation (2.34) for the diffuse transmission is more difficult. It is helpful to first rewrite (2.34) in terms of the total transmission and obtain the analytic solution of the total transmission equation. The diffuse transmission solution is then obtained by subtracting the uncollided component. The total transmission equation analogous to (2.34) is

$$\begin{aligned} \frac{d}{ds} T_t(s) &= \sigma C g(-1,1) T_t(s) - \sigma T_t(s) + \\ &\quad \frac{1}{2} R(s) \sigma C g(1,-1) T_t(s) \end{aligned} \quad (2.41)$$

where the initial condition is now

$$T_t(0) = 2. \quad (2.42)$$

The solutions of (2.41) and (2.34) can be expressed in terms of the reflection in the forms

$$T_t(s) = \sqrt{A^2 - 1} \operatorname{csch}(Bs) R(s) \quad (2.43)$$

and

$$T(s) = T_t(s) - 2 \exp(-\sigma s) . \quad (2.44)$$

Slightly less restrictive assumptions can be made. In particular, instead of assuming that a particle is always scattered straight forward or straight backward, an average value of the direction cosine could be used. The restriction to a homogeneous medium could also be relaxed if desired (to discrete layers).

Discussion

An equation for the total transmission is obtained by deleting the two terms containing exponential factors from (2.32) and changing the initial condition to

$$T_t(0, \mu, E; \mu', E') = 2\mu \delta(\mu - \mu') \delta(E - E') . \quad (2.45)$$

The derivation of this chapter was in terms of the diffuse transmission even though the resulting equation is more complicated. The angular distribution of the total transmission is very anisotropic at small thicknesses because of the delta function initial condition whereas the angular distribution of the diffuse transmission is relatively smooth in the region. This leads one to suspect that a less accurate angular approximation may be needed for the calculation of the diffuse transmission than for the total transmission near the origin.

CHAPTER III
NUMERICAL SOLUTION OF THE REFLECTION
AND TRANSMISSION EQUATIONS

Introduction

The plane geometry reflection and transmission equations derived in Chapter II are rigorous but cannot be solved because of the integral terms. As the first step in the numerical solution of these equations, the integrals are approximated by finite sums thereby obtaining a finite set of coupled first-order nonlinear ordinary differential equations. The solution of this system of equations by ordinary methods such as the Runge-Kutta and the Adams methods is then discussed. Finally, a systematic method of deriving numerical methods for the solution of differential equations based upon exponential approximations is introduced and the application of the most successful of these methods to the reflection and transmission equations is given.

The numerical solutions based upon approximations that are exact for exponentials which are discussed in this chapter would seem to be useful in many other applications in which it is known from the physics of the problem that exponential behavior is to be expected.

Reduction to a Finite Set of Differential Equations

In order to solve equations (2.31) and (2.32) numerically, the integral terms are replaced by finite sums of the form

$$f(x) = \sum_{k=1}^m w_k f(x_k) \quad (3.1)$$

where the abscissas x_k and weights w_k are to be chosen in accordance

with the particular numerical integration formula chosen. The discrete form of (2.31) is

$$\begin{aligned}
 \frac{d}{dx} R(I, J) = & \\
 & 2 \sigma(J) C(J) p(I, J) + \\
 & \sum_{K=1}^N W(K) \sigma(J) C(J) p(K, J) R(I, K) - \\
 & \left[\frac{\sigma(I)}{\mu(I)} + \frac{\sigma(J)}{|\mu(J)|} \right] R(I, J) + \\
 & \sum_{L=N+1}^{2N} W(L) R(L, J) \sigma(L) C(L) p(I, L) + \\
 & \frac{1}{2} \sum_{K=1}^N W(K) \sum_{L=N+1}^{2N} W(L) R(L, J) \sigma(L) C(L) p(K, L) R(I, K) \quad (3.2)
 \end{aligned}$$

where the slab thickness is now x instead of s , N is the number of particle states, p is the state-to-state transfer probability analogous to (2.13) (see Appendix A for definition), $\mu(I)$ is the direction cosine assigned to state I , $W(I)$ is the product of the energy and angular integration formula weights divided by the absolute value of the direction cosine for state I , and all quantities are functions of position except the numerical integration (quadrature) formula abscissas and weights W .

The number of particle states, N , is defined as the product of the number of discrete energy values used in the energy integrations and the number of discrete direction cosines used in the angular integrations over $(-1, 0)$ and $(0, 1)$. Particle states from 1 to N have all

possible energies combined with all possible positive direction cosines. The particle direction is reversed without change in energy group by adding or subtracting N from the state index. J is the incident particle state index ($1 \leq J \leq N$) and I is the exit particle state index ($N+1 \leq I \leq 2N$).

Defining

$$S(I, J) = W(I)W(J) \sigma(J)C(J)p(I, J) \quad (3.3)$$

the discrete form of the reflection equation becomes

$$\begin{aligned} \frac{d}{dx} R(I, J) = & \frac{2}{W(I)W(J)} S(I, J) + \\ & W\left(\frac{1}{J}\right) \sum_{K=1}^N R(I, K)S(K, J) - \left[\frac{\sigma(I)}{\mu(I)} + \frac{\sigma(J)}{|\mu(J)|} \right] R(I, J) + \\ & \frac{1}{W(I)} \sum_{L=N+1}^{2N} S(I, L)R(L, J) + \frac{1}{2} \sum_{K=1}^N \sum_{L=N+1}^{2N} R(I, K)S(K, L)R(L, J). \end{aligned} \quad (3.4)$$

Equation (3.4) represents a coupled set of N^2 first-order nonlinear ordinary differential equations subject to the initial condition

$$R(I, J) = 0 \quad (3.5)$$

at $x = 0$ for all I and J .

The corresponding discrete form transmission equation is

$$\begin{aligned} \frac{d}{dx} T(I, J) = & - \frac{\sigma(J)}{|\mu(J)|} T(I, J) + \\ & \frac{1}{W(I)} \exp \left[- \frac{1}{|\mu(I)|} \int_0^x \sigma(I) dx' \right] \left[\frac{2}{W(J)} S(I, J) + \sum_{L=N+1}^{2N} S(I, L)R(L, J) \right] \\ & + \frac{1}{W(J)} \sum_{K=1}^N T(I, K)S(K, J) + \frac{1}{2} \sum_{K=1}^N \sum_{L=N+1}^{2N} T(I, K)S(K, L)R(L, J) \end{aligned} \quad (3.6)$$

where the exit particle state index, I , for transmitted particles is in $(1,N)$ and the initial condition is

$$T(I,J) = 0 \quad (3.7)$$

at $x = 0$ for all I and J .

The remaining integral over the total cross section for the exit transmitted state, $\sigma(I)$, in (3.6) is to be evaluated by assuming that the total cross section varies in a stepwise manner, i.e., that the slab is composed of discrete layers so that the composition does not vary with position within a layer. Defining the uncollided component of the transmitted flux in the general case as

$$T_u(x,I) = \frac{2}{W(I)} \exp \left[- \frac{1}{|\mu(I)|} \int_0^x \sigma(I) dx' \right], \quad (3.8)$$

in the case of discrete layers the uncollided component becomes

$$T_u(x+h,I) = T_u(x,I) \exp \left[- \frac{\sigma(I)}{|\mu(I)|} h \right] \quad (3.9)$$

with initial condition

$$T_u(0,I) = 2/W(I). \quad (3.10)$$

Transmission equation (3.6) can now be rewritten using the above definition of the uncollided component of the transmitted flux in the form

$$\begin{aligned}
\frac{d}{dx} T(I, J) &= - \frac{\sigma(J)}{|\mu(J)|} T(I, J) + \\
T_u(I) &\left[\frac{S(I, J)}{W(J)} + \frac{1}{2} \sum_{L=N+1}^{2N} S(I, L) R(L, J) \right] + \\
\frac{1}{W(J)} \sum_{K=1}^N T(I, K) S(K, J) &+ \frac{1}{2} \sum_{K=1}^N \sum_{L=N+1}^{2N} T(I, K) S(K, L) R(L, J) \quad (3.11)
\end{aligned}$$

where the dependence of T_u upon x has been suppressed in order to be consistent with the notation for the diffuse transmission T .

The discrete form total transmission equation is

$$\begin{aligned}
\frac{d}{dx} T_t(I, J) &= - \frac{\sigma(J)}{|\mu(J)|} T_t(I, J) + \\
\frac{1}{W(J)} \sum_{K=1}^N T_t(I, K) S(K, J) &+ \frac{1}{2} \sum_{K=1}^N \sum_{L=N+1}^{2N} T_t(I, K) S(K, L) R(L, J) \quad (3.12)
\end{aligned}$$

with initial condition

$$T_t(I, J) = \begin{cases} 0 & \text{when } I = J \\ 2/W(I) & \text{otherwise.} \end{cases} \quad (3.13)$$

Comparison of equations (3.11) and (3.12) for the diffuse and total transmission, respectively, shows that while the diffuse transmission equation is more complicated, the additional effort required is small compared to the effort required to evaluate the double sum term which appears in both equations.

Solution by Means of Ordinary Methods

Equations (3.4) and (3.11) for the reflection and diffuse transmission constitute a set of $2(N)^2$ coupled first-order differential equations. A multitude of methods for the solution of such equations are available in the literature on numerical analysis [9, 10]. The application of two of the most widely used methods will be discussed in this section.

A fourth-order Runge-Kutta method was tried first. The Runge-Kutta methods have the advantage of being both self-starting and relatively stable. The Runge-Kutta methods were eventually discarded because:

1) more than evaluation of the right-hand-side of the differential equation is required at each step and this is very time consuming in this problem due to the double sum on the right-hand-side of (3.4) and (3.11) or (3.12), and 2) it is difficult to estimate the truncation error per step.

Next a fourth-order Adams method based on the FORTRAN Monitor System library subprogram INDV, DPNV [29] was used. The Adams method requires only one evaluation of the right-hand-side of the differential equation at each step and the truncation error per step may be relatively easily estimated. The method is not self-starting so that special starting equations are required and a large amount of fast memory space is required. In addition double precision operations are required at one point in the Adams method to control the growth of round off error due to subtraction of nearly equal numbers from each other.

In summary, the Runge-Kutta method was easy to apply but was

very slow and lacked an easy method of estimating the truncation error per step, and the Adams method while much faster with easy estimate of the truncation error per step required an excessive amount of core storage and special starting equations making changes in step size more difficult.

Solution By Means of Exponential Approximations

The reflection and transmission matrices can be expected on physical grounds to approach simple exponential growth or decay in each element as the thickness of a shield layer increases. Thus it is reasonable to investigate approximations that would be exact for simple exponential functions as alternatives to the polynomial approximations of the last section. This approach was, in part, motivated by the work of Hansen, Koen, and Little [11] and Certainé [12] on numerical solutions of the reactor kinetics equations.

The following systematic approach may be used to generate many different types of exponential approximations together with error estimates for the procedures. Let the differential equation be given by

$$y' (x) = f(x,y) \quad (3.14)$$

with initial condition

$$y(x_0) = y_0 \quad (3.15)$$

Let

$$\begin{aligned}x_n &= x_0 + nh & n &= 0, 1, 2, \dots \\y_n &= y(x_n) \\f_n &= f(x_n, y_n)\end{aligned}\tag{3.16}$$

and

$$w_n = w(x_n)\tag{3.17}$$

where $w(x)$ is an as yet unspecified weight function.

Subtract $w_r y(x)$ from both sides of (3.14), multiply both sides by $\exp(-w_r x)$, and integrate from x_a to x_b to obtain

$$\int_{x_a}^{x_b} [y'(x) - w_r y(x)] \exp(-w_r x) dx = \int_{x_a}^{x_b} [f(x, y) - w_r y(x)] \exp(-w_r x) dx\tag{3.18}$$

The left-hand-side of (3.18) is a perfect differential and may be readily integrated to give

$$y_b = \exp[w_r(b-a)h] y_a + \exp w_r x_b \int_{x_a}^{x_b} [f(x, y) - w_r y(x)] \exp(-w_r x) dx.\tag{3.19}$$

Equation (3.19) is exact. The integral term in (3.19) will now be approximated in various manners. A first-order exponential approximation results if the simple Euler approximation

$$\int_{x_r}^{x_{r+s}} f(x) dx = (sh) f_r + \frac{(sh)^2}{2} f'(u)\tag{3.20}$$

where $x_r < u < x_{r+s}$, is used to approximate the integral in (3.19) so that

$$y_{r+s} = \exp(shw_r) \left[y_r + h (f_r - w_r y_r) \right] + \frac{(sh)^2}{2} \exp(w_r x_{r+s}) I'(u) \quad (3.21)$$

where

$$I(x) = [f(x, y) - w_r y(x)] \exp(-w_r x). \quad (3.22)$$

One can now define the weight function as

$$w(x) = f(x, y) / y(x) = y'(x) / y(x) \quad (3.23)$$

so that the term containing $f_r - w_r y_r$ in (3.21) will be zero and (3.21) becomes

$$y_{r+s} = \exp(shw_r) y_r + \frac{(sh)^2}{2} \exp(w_r x_{r+s}) I'(u). \quad (3.24)$$

The first-order approximation (3.24) is the exponential equivalent of Euler's method. It is remarkably simple but exact for an exponential dependence of y on the independent variable x .

A second-order exponential approximation results if the trapezoidal rule

$$\int_{x_r}^{x_{r+s}} I(x) dx = \frac{sh}{2} [I_r + I_{r+s}] - \frac{(sh)^3}{12} I''(u) \quad (3.25)$$

is used to approximate the integral in (3.19) so that

$$y_{r+s} = \exp(shw_r) y_r + \exp(w_r x_{r+s}) \left[\frac{sh}{2} I_{r+s} - \frac{(sh)^3}{12} I'''(u) \right] \quad (3.26)$$

The second-order exponential approximation (3.26) which was obtained by means of the trapezoidal rule is an implicit equation in that the value of I_{r+s} depends upon the unknown value of y_{r+s} that is being sought.

When s is even, and the midpoint rule

$$\int_{x_{r-s/2}}^{x_{r+s/2}} I(x) dx = (sh)I_r + \frac{(sh/2)^3}{3} I(v) \quad (3.27)$$

where $x_{r-s/2} < v < x_{r+s/2}$ is used, then (3.19) becomes

$$y_{r+s/2} = \exp(shw_r) y_{r-s/2} + \exp(w_r x_{r+s/2}) \frac{(sh/2)^3}{3} I'''(v). \quad (3.28)$$

The second-order exponential approximation (3.28) is a very simple explicit equation that can be used to predict the new value of y .

Equations (3.26) and (3.28) can be combined so as to yield an error estimate for the second order exponential approximation. If $s=2$ is used in (3.28) the predicted value of y at x_{r+1} is

$$y_{r+1}^p = \exp(2hw_r) y_{r-1} \quad (3.29)$$

where the superscript p denotes a predicted value, and if $s=1$ is used in (3.26) the corrected value of y at x_{r+1} is

$$y_{r+1}^c = \exp(hw_r) y_r + \exp(w_r x_{r+1}) \frac{h}{2} (f_{r+1} - w_r y_{r+1}^p). \quad (3.30)$$

where the superscript c denotes a corrected value. Now make the assumption that, for small enough h , the second derivative terms in (3.26) and (3.28) are approximately equal and solve for the approximate error per step when the second-order predictor-corrector pair (3.29) and (3.3) are used in the form

$$y_{r+1} - y_{r+1}^c = \frac{y_{r+1}^c - y_{r+1}^p}{5} \quad (3.31)$$

which is entirely analogous to the usual relation for polynomial approximations [9] .

The error estimate for the first-order exponential predictor

$$y_{r+1}^p = \exp(h w_r) y_r \quad (3.32)$$

obtaining by ignoring the error term in (3.24) is

$$E_{r+1} = \frac{h^2}{2} \exp(w_r x_{r+1}) \left[\frac{d}{dx} (f(x, y) - w_r y(x)) \exp(-w_r x) \right]_{x=u} \quad (3.33)$$

where $x_r < u < x_{r+1}$. This error may be estimated by

$$E_{r+1} = -\frac{h^2}{2} w_r (w_{r+1} - w_r) \exp(w_r h) y_r \quad (3.24)$$

so that the approximate relative error in y_{r+1} compared to y_r when

the first-order exponential approximation (3.32) is used is

$$RE_{r+1} = \frac{E_{r+1}}{r_{r+1}} = -\frac{h^2}{2} w_r (w_{r+1} - w_r) \quad (3.35)$$

Both the first and second order exponential approximations were tried. In practice the second order procedure was not as good as the first order procedure because of a tendency of the second order procedure toward a type of instability in which alternate steps diverge in opposite directions from the true solution and the loss of flexibility because the second order procedure is not self starting.

The final version of the numerical solution of the plane geometry reflection and transmission equations was therefore based upon the first order exponential predictor (3.32) with the stepwise error estimate (3.35). When applying these exponential approximations to the reflection and diffuse transmission equations (3.4) and (3.11), one must be careful to define suitable weighting functions. Because of the zero initial condition, the right-hand-sides of differential equations (3.4) and (3.11) must be split into vanishing and nonvanishing terms. Fortunately, the nonvanishing terms may be integrated analytically. This is a major factor in the stability of these numerical procedures particularly in the case of the reflection equation in which the nonvanishing term is always of the same order of magnitude as the term which vanishes at the origin.

Rewrite equation (3.4) in the form

$$\frac{d}{dx} R(x, I, J) = B(x, I, J) + K_p(x, I, J) \quad (3.36)$$

where

$$B(x, I, J) = \frac{2}{W(I)W(J)} S(I, J) \quad (3.37)$$

and $K_r(x, I, J)$ is the rest of the right-hand-side of (3.4). Because each term of $K_r(x, I, J)$ contains $R(x, I, J)$ as a factor

$$R(0, I, J) = K_r(0, I, J) = 0 \quad (3.38)$$

and

$$W_r(x, I, J) = K_r(x, I, J)/R(x, I, J) \quad (3.39)$$

is finite at the origin.

Following the same procedure as before, one obtains in the first order exponential approximation

$$R(x, I, J) = \exp \left[W_r(x, I, J) h \right] R(x, I, J) + \exp \left[W_r(x, I, J) (x+h) \right] \int_x^{x+h} B(s, I, J) \exp \left[-W_r(x, I, J) s \right] ds \quad (3.40)$$

Now, if $B(s, I, J)$ is a constant in the interval $s = x$ to $s = x+h$ (i.e., a slab composed of discrete layers) equation (3.40) can be integrated to give

$$R(x+h, I, J) = \exp \left[W_r(x, I, J) h \right] R(x, I, J) + \left[B(x, I, J)/W_r(x, I, J) \right] \left(\exp \left[W_r(x, I, J) h \right] - 1 \right) \quad (3.41)$$

with relative error estimate

$$E_r = -\frac{h^2}{2} W_r(x) \left[W_r(x+h) - W_r(x) \right] \quad (3.42)$$

in which the particle state indices have been suppressed for clarity.

Equation (3.11) for the diffuse transmission is rewritten in

the form

$$\frac{d}{dx} T(x, I, J) = F_1(x, I, J) + K_t(x, I, J) \quad (3.43)$$

where

$$F_1(x, I, J) = \frac{S(I, J)}{W(J)} T_u(x, I) \quad (3.44)$$

and $K_t(x, I, J)$ is the rest of the right-hand-side of (3.11). As in the reflection case

$$T(0, I, J) = K_t(0, I, J) = 0 \quad (3.45)$$

and

$$W_t(x, I, J) = K_t(x, I, J)/T(x, I, J) \quad (3.46)$$

is finite at the origin.

Applying the first-order exponential approximation to the diffuse transmission equation written in this form yields

$$T(x+h, I, J) = \exp[W_t(x, I, J)h] T(x, I, J) + \left[\exp[W_t(x, I, J)(x+h)] \int_x^{x+h} F_1(s, I, J) \exp[-W_t(x, I, J)s] ds \right]. \quad (3.47)$$

In the case of discrete layers with constant properties in the interval $(x, x+h)$ one can write

$$F_1(s, I, J) = F(x, I, J) T_u(x, I) \exp\left[-\frac{\sigma(I)}{|\mu(I)|} (s-x)\right] \quad (3.48)$$

where

$$F(x, I, J) = \frac{S(I, J)}{W(J)} \quad (3.49)$$

and (3.47) can be integrated to yield

$$T(x+h, I, J) = \exp[W_t(x, I, J)h]T(x, I, J) + \frac{F(x, I, J)T_u(x, I)}{W_t(x, I, J) + \frac{\sigma(I)}{|\mu(I)|}} \left(\exp[W_t(x, I, J)h] - \exp\left[-h \frac{\sigma(I)}{|\mu(I)|}\right] \right) \quad (3.50)$$

with relative error estimate

$$E_t = - \frac{h^2}{2} W_t(x) [W_t(x+h) - W_t(x)] \quad (3.51)$$

where the particle state indices have been suppressed for clarity.

Because the uncollided component of the transmission, T_u , eventually becomes negligible with respect to the scattered component, T , at large thicknesses the transmission equation (3.50) tends to become simply

$$T(x+h, I, J) = \exp[W_t(x, I, J)h]T(x, I, J) \quad (3.52)$$

that is, the stabilizing effect of the analytically integrated term decreases as the attenuation increases.

A large amount of analytic and experimental effort was expended on the question of the numerical stability of these approximations. The results may be summed up quite simply.

The numerical solution of the reflection equation is stable for all step sizes in the range of interest provided that the reflection calculation is terminated and the reflection set to a constant value for the remainder of the region when the derivative of the reflection with respect to the slab thickness x becomes less than 0.001 to 0.0001. This is not restrictive since such a cutoff is highly desirable to speed up the computation.

The numerical solution of the transmission equation is unstable for step sizes larger than a quantity that is of the same order of magnitude as the partial derivative of the right-hand-side of the differential equation (3.11) with respect to the transmission variable. An estimate of this quantity that has been used successfully may be obtained by dividing the smallest direction cosine used in the angular integrations by the largest value of the total macroscopic cross section used in the problem.

Since larger step sizes can be allowed in the numerical solution of the reflection equation than for the transmission, and the transmission equation is much simpler to evaluate for a constant reflection, it was found advantageous to use separate step sizes for the reflection and transmission equations. The reflection step size was allowed to assume some integral multiple of the transmission step size if the stepwise error estimate for the reflection was smaller than the error estimate for the transmission or if the transmission step size was restricted to a smaller value because of the stability limit.

Equations (3.42) and (3.51) for the stepwise error estimates show that the step size should be adjusted in proportion to the square root of the ratio of the desired stepwise error criterion to the estimated stepwise error. In practice it was found better to use the third root to eliminate or strongly damp any tendency to overshoot and oscillate about the desired step size.

Discussion

Successful numerical solutions of the reflection and transmission equations were obtained by all four of the methods described as well as a few other variations not described here. Most of the solutions were too slow to allow realistic energy dependent problems to be solved in a reasonable length of time. The exponential approximations were introduced in order to take advantage of the physics of this particular problem and proved to be quite useful.

The first computer program used the Runge-Kutta method and was written in the FORTRAN programming language. Later programs were written in the MAD programming language and designed for use with the M. I. T. time sharing system as well as the normal IBM 7094 batch processing. One version of the MAD program using the Adams method used FORTRAN double precision subroutines in an effort to reduce the problem of numerical instability encountered with this method. This effort was not successful and the method was abandoned.

The final version of the computer program based upon equations (3.41) and (3.51) named "Program STAR" where STAR stands for "Slab Transmission and Reflection" is described in Appendix C.

CHAPTER IV

RESULTS

Introduction

Four problems have been selected to illustrate the application of the invariant imbedding method. The problems are presented in order of increasing complexity. The first problem is a simple rod model restricted to monoenergetic particles with a very special scattering law. It is included because an analytic solution is possible. The second problem is a slab shield in which all particles have the same energy and the scattering is isotropic in the laboratory coordinate system. This problem is included because solutions are available in the astrophysical literature [2, 13]. The third problem is a slab shield composed of water with a plane isotropic fission source of unit strength located at one face. The results are converted to a point source geometry and compared with the extensive computations published by the Shielding Division of the American Nuclear Society [14]. The fourth problem is a slab shield composed of alternating layers of iron and polyethylene with a plane isotropic fission neutron source of unit strength located at one face. The results are compared with those of Alen et al. [15]. Finally, the computing time required for these problems is discussed.

The invariant imbedding method results presented in this chapter were obtained from a computer program named STAR which solves the plane geometry invariant imbedding equations using the first-order exponential approximation described in Chapter III. Program STAR is described in detail in Appendix C.

The definition of the relative error in percent used throughout this chapter is

$$\text{R. E. in \%} = \frac{\text{True Value} - \text{Approximate Value}}{\text{True Value}} \times 100\% \quad (4.1)$$

where the true value is to be taken as the data to which the program STAR result is being compared unless otherwise noted.

Monoenergetic particles in a thin rod. The model for which the analytic solution discussed in Chapter II is valid can be described as a thin rod or wire with source particles incident upon one end and constrained to move only along the axis of the rod without change in energy. A short computer program named ANSOL was written to obtain precise values of the analytic solutions of the reflection and transmission equations for this model.

Analytic and program STAR results for a rod model problem in which the scattering was isotropic and the mean number of secondaries per collision, C , was 0.9 are presented in Figure 3, Figure 4, Table I, and Table II. The results are in terms of the reflection and transmission variables used in Chapters II and III. The reflected and transmitted scalar fluxes for this problem with a source of unit strength located at one end of the rod ($\frac{1}{2}$ of source incident upon the rod) would be one-fourth of the reflection and transmission variables presented here (see Appendix B for relations between the reflection and transmission variables and other quantities of interest.)

These results are typical of the behavior of the reflection and transmission in more complex problems. The reflection asymptotically approaches a constant value in a homogeneous region and the diffuse and total transmission approach the same exponential attenuation with increasing length or thickness.

Note that the relative error in the reflection decreases as the reflection approaches the asymptotic value, but that the error in the transmission accumulates. The accumulated error in the transmission is not serious. The same problem was continued to a rod length of 210.0 at which point the transmission was $2.070\text{E-}29$ with 1.85% relative error compared to the analytic solution value of $2.109\text{E-}29$.

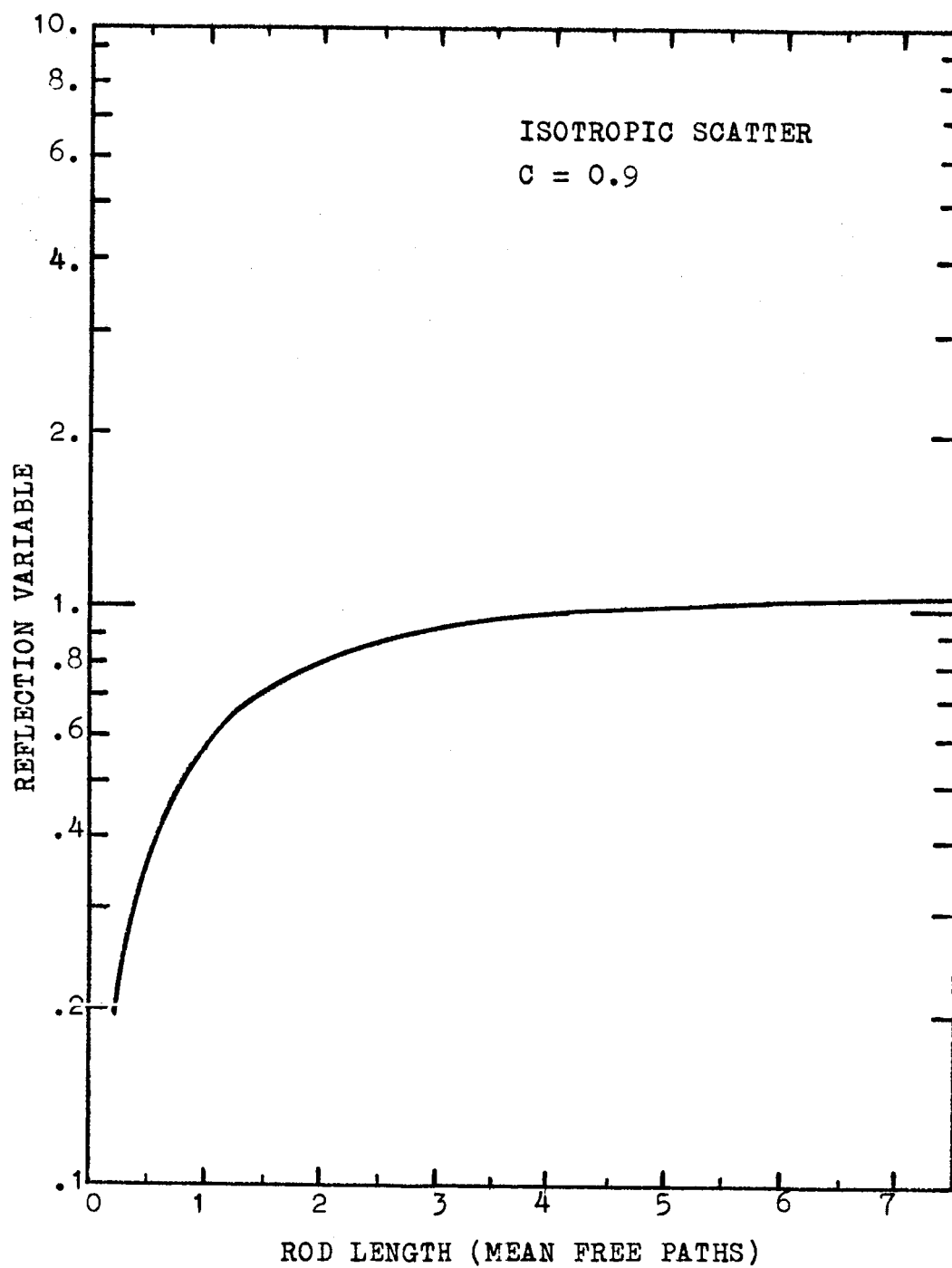


FIGURE 3
REFLECTION VERSUS ROD LENGTH

TABLE I
REFLECTION VALUES FOR ROD MODEL WITH
ISOTROPIC SCATTER AND $C = 0.9$

Rod Length (Mean Freepaths)	Reflection From Analytic Solution	Reflection From Program STAR	Relative Error (In Percent)
0.	0.	0.	0.
0.25	0.19744	0.19743	0.005
0.50	0.35065	0.35060	0.014
0.75	0.47164	0.47155	0.019
1.00	0.56850	0.56837	0.023
1.25	0.64690	0.64675	0.023
1.50	0.71094	0.71077	0.024
1.75	0.76361	0.76344	0.023
2.00	0.80721	0.80702	0.023
2.25	0.84346	0.84328	0.021
2.50	0.87374	0.87356	0.021
2.75	0.89911	0.89893	0.020
3.00	0.92043	0.92026	0.019
3.50	0.95355	0.95340	0.016
4.00	0.97722	0.97709	0.013
5.00	1.00651	1.00642	0.009
6.00	1.02182	1.02176	0.006
7.00	1.02990	1.02986	0.004
8.00	1.03416	1.03414	0.002
9.00	1.03643	1.03641	0.002
10.00	1.03763	1.03762	0.001

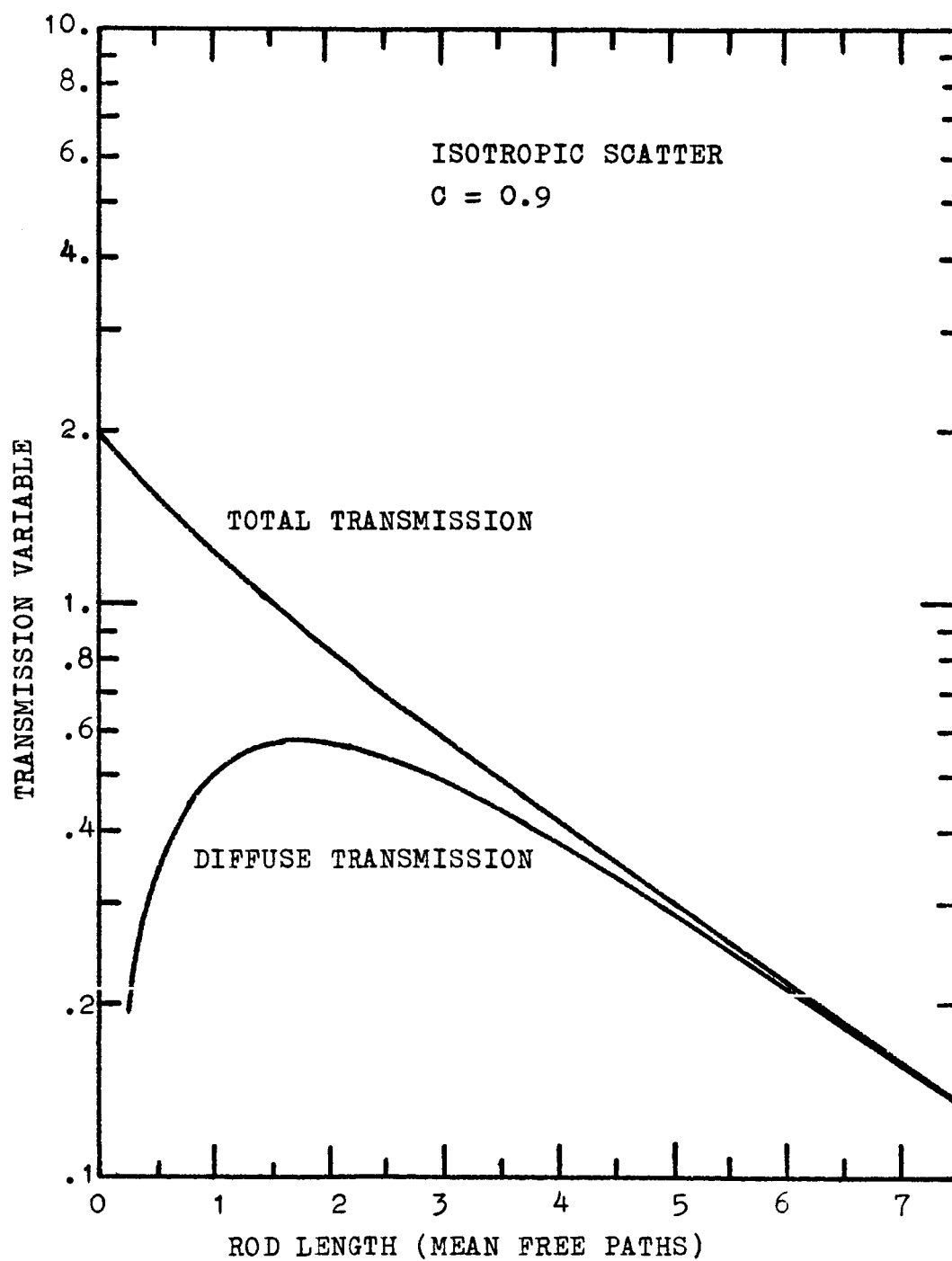


FIGURE 4
TRANSMISSION VERSUS ROD LENGTH

TABLE II
TRANSMISSION VALUES FOR ROD MODEL WITH
ISOTROPIC SCATTER AND $C = 0.9$

Rod Length (Mean Free Paths)	Diffuse Transmission From Analytic Solution	Diffuse Transmission From Program STAR	Relative Error (In Percent)
0.	0.	0.	0.
0.25	0.19560	0.19546	0.072
0.50	0.33892	0.33878	0.041
0.75	0.43970	0.43961	0.021
1.00	0.50676	0.50675	0.002
1.25	0.54763	0.54769	-0.011
1.50	0.56850	0.56861	-0.019
1.75	0.57434	0.57450	-0.028
2.00	0.56911	0.56930	-0.033
2.25	0.55590	0.55611	-0.038
2.50	0.53712	0.53734	-0.041
2.75	0.51460	0.51483	-0.044
3.00	0.48976	0.48999	-0.046
3.50	0.43706	0.43728	-0.049
4.00	0.38461	0.38480	-0.051
5.00	0.29043	0.29058	-0.052
6.00	0.21537	0.21548	-0.053
7.00	0.15831	0.15839	-0.053
8.00	0.11587	0.11593	-0.052
9.00	0.084633	0.084677	-0.052
10.00	0.061751	0.061783	-0.052

Monoenergetic particles in an isotropically scattering medium.

The second problem considers a slab shield composed of some hypothetical material that scatters particles isotropically in the laboratory coordinate system without changing the energy of the particle.

The reflection values for seven angular groups were compared with the reflection values tabulated by Bellman, et al. [13]. It was necessary to divide the reflection by four times the cosine of the exit direction in order to obtain the same reflection variable tabulated by Bellman. The relative error between the two sets of values was always less than 1.5%. Most of the difference appeared to be due to the fact that the program STAR results do not generally come out at exactly even values of the thickness due to the variable step size feature.

The X and Y functions defined by Chandrasekhar and tabulated by Mayers [16] were used to compute values of the reflection and transmission from the relations

$$R(t, u, v) = \frac{uv}{u+v} C \left[X(t, u)X(t, v) - Y(t, u)Y(t, v) \right] \quad (4.2)$$

and

$$T(t, u, v) = \frac{uv}{u-v} C \left[Y(t, u)X(t, v) - X(t, u)Y(t, v) \right] \quad (4.3)$$

where t is the slab thickness in mean free paths, u and v are the exit and incident direction cosines respectively, and C is the mean number of secondaries per collision.

The values of the reflection and transmission array elements computed by program STAR were within 2% of the values calculated from the X and Y functions at both 1 and 5 mean free paths. Most of the values differed by much less than 2%. Examination of the results showed

that the larger differences were in the smaller values of the transmission for which the difference of two nearly equal numbers is required in the calculation of the transmission from the X and Y functions.

The X and Y function tables were also used to calculate the reflected and diffusely transmitted currents according to the relations

$$J_0(t) = -\frac{1}{4} \int_0^1 du \int_0^1 dv \frac{uv}{u+v} C [X(t,u)X(t,v) - Y(t,u)Y(t,v)] \quad (4.4)$$

and

$$J_X(t) = \frac{1}{4} \int_0^1 du \int_0^1 dv \frac{uv}{u-v} C [Y(t,u)X(t,v) - X(t,u)Y(t,v)] \quad (4.5)$$

where J_0 and J_X are the reflected and transmitted currents, respectively, due to a unit isotropic source.

The reflected and transmitted currents were within 0.5% at 1 mean free path and within 0.2% at 5 mean free paths.

The question of how the number of angular groups affects the calculated transmission values was checked by running two series of problems that were identical except for the number of angular subdivisions employed in program STAR.

Figure 5 presents the results of the first series in the form of the net transmitted flux as a function of the incident direction and the number of angular groups. It is apparent that the particles which are incident close to the normal are the most likely to be transmitted and that two or three angular groups are adequate for these particles (the minimum number of angular groups that may be employed without the introduction of adjustable constants is two).

Figure 6 presents the transmitted current for a unit isotropic source as a function of the number of angular groups. Again, it is apparent that two or three angular groups are sufficient, particularly when it is noted that the attenuation in Figure 6 amounts to some 13

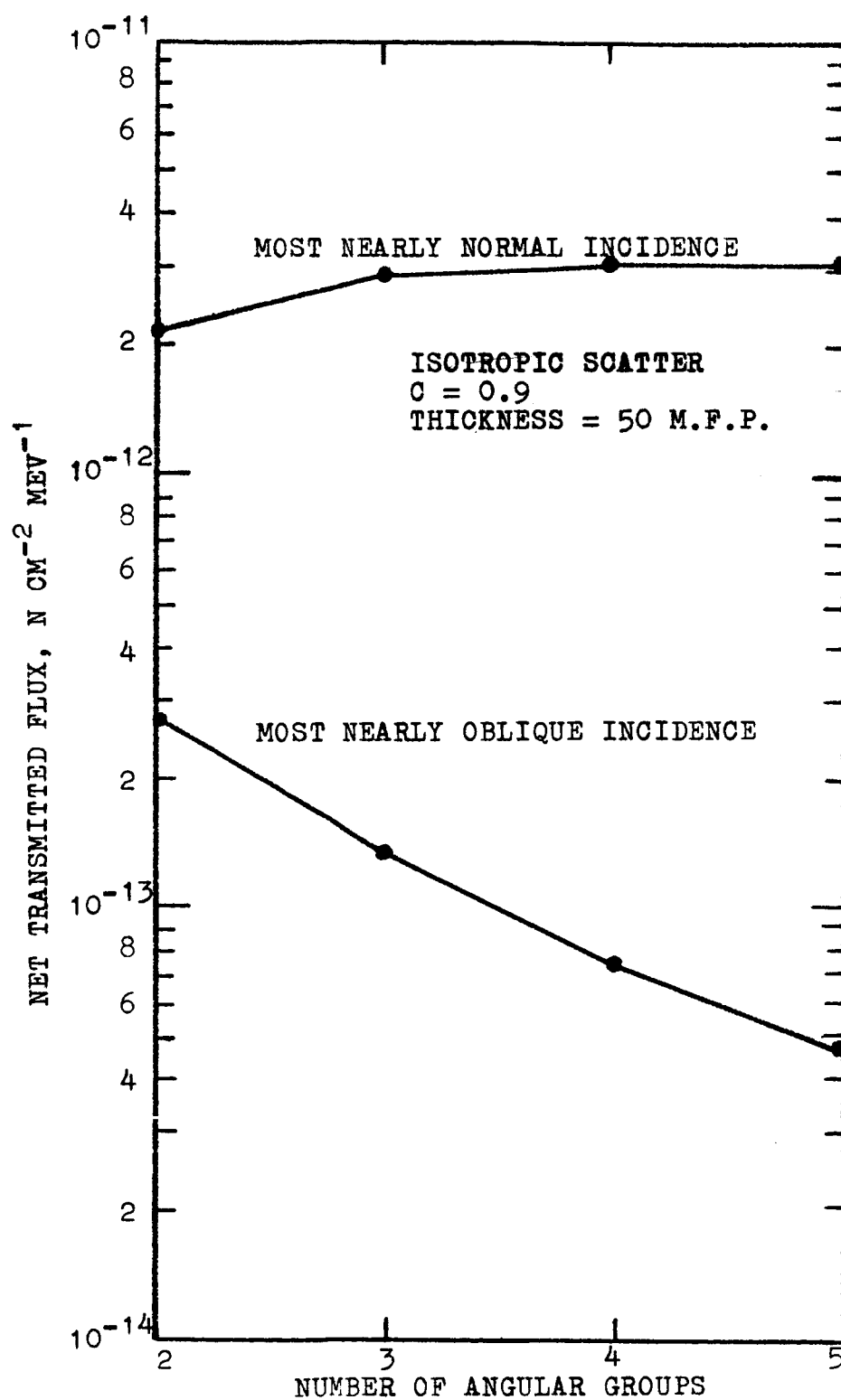


FIGURE 5
NET TRANSMITTED FLUX VERSUS NUMBER OF
ANGULAR GROUPS AND INCIDENT DIRECTION

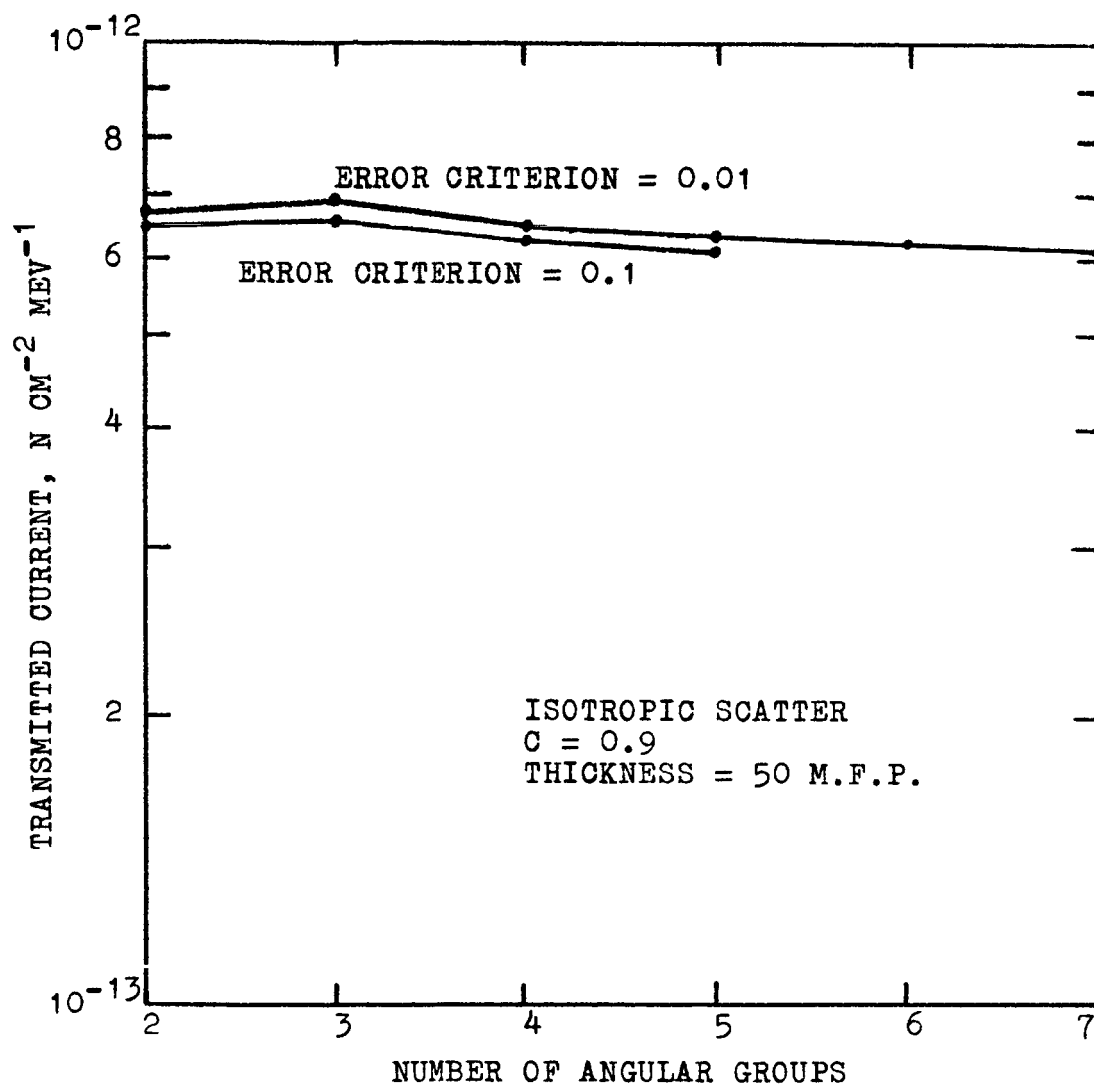


FIGURE 6
TRANSMITTED CURRENT DUE TO A UNIT ISOTROPIC
SOURCE VERSUS THE NUMBER OF ANGULAR GROUPS

powers of ten.

Since program STAR continuously adjusts the step size to keep the estimated truncation error per step close to an error criterion that is an input variable to the program, it is very important to investigate the effect of this error criterion upon the calculated results. Fortunately, as Figure 7 shows, the transmitted current is relatively insensitive to the value of the error criterion. The reason for this is that there is a limitation on the maximum step size imposed by the requirements for stability which apparently prevents the step size from growing to the point where serious error is introduced. Values of the error criterion greater than 0.1 were also investigated. It was found that the error control procedure began to fail for values much larger than 0.1.

The question of how small changes or uncertainties in the input data affect the calculated transmission values was investigated by running a series of problems with systematic variations in the value of the mean number of secondaries per collision, C , and in the error criterion. The results are summarized in Table III.

The effect of the change in the error criterion varies with the value of C , being about 0.1 to 0.2% at $C=0.5$, 4 to 5% at $C=0.9$, and about 16% at $C=0.99$.

The effect of changes in the value of C may be described more easily in terms of the changes in the quantity $(1 - C)$. A change of 1% in $(1 - C)$ leads to a change of 7 to 9% in the transmitted current. It should be noted that a 1% change in $(1 - C)$ near $C=0.99$ amounts to only a 0.01% change in the value of C itself, so that this type of

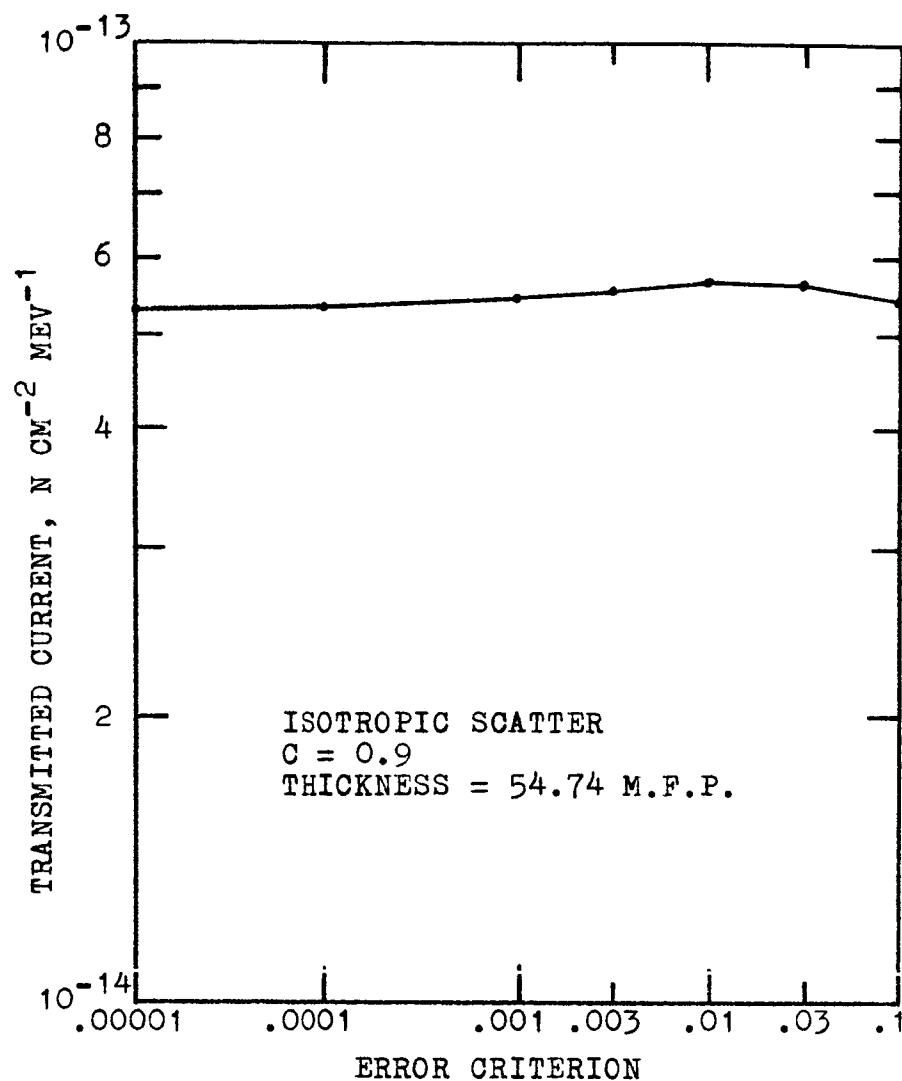


FIGURE 7
TRANSMITTED CURRENT DUE TO A UNIT ISOTROPIC
SOURCE VERSUS THE ERROR CRITERION

TABLE III
EFFECT OF CHANGES IN C AND THE ERROR CRITERION
(THREE ANGULAR GROUPS USED)

Mean Number Of Secondaries Per Collision	Error Criterion	Slab Thickness (Mean Free Paths)	Reflected Current (N-CM ⁻² -MEV ⁻¹)	Transmitted Current (N-CM ⁻² -MEV ⁻¹)
0.5	0.1	20.05	-.036671	4.719E-10
0.5	0.01	20.05	-.036671	4.729E-10
0.495	0.1	20.05	-.036135	4.465E-10
0.495	0.01	20.05	-.036135	4.460E-10
0.9	0.1	40.09	-.119506	1.191E-10
0.9	0.01	40.09	-.119500	1.254E-10
0.899	0.1	40.09	-.119046	1.089E-10
0.899	0.01	40.09	-.119041	1.138E-10
0.99	0.1	100.08	-.198254	2.129E-09
0.99	0.01	100.08	-.198467	2.537E-09
0.9899	0.1	100.08	-.198037	1.975E-09
0.9899	0.01	100.08	-.198248	2.345E-09

problem will be extremely sensitive to small changes in the input data when the absorption is small and C is close to unity.

Polyenergetic neutrons in water. The third problem is a much more realistic problem in which energy and direction dependent cross sections are used. Reflection and transmission values were computed for neutrons incident upon a slab shield composed of water.

The cross sections for neutron interactions with water were taken from either the report on moments method calculations in water by Aronson et al. [17] or from the cross sections prepared by Goldstein for the Shielding Division of the American Nuclear Society (hereafter referred to as the S. D. of the A. N. S.) [18]. This microscopic neutron cross section data was then converted into the desired form for input to program STAR (see Appendices A and D for details).

The neutron transmission values were converted into neutron fluxes and doses due to a unit isotropic fission source as part of the output section of program STAR (see Appendix B for details). The doses and an occasional flux versus energy plot were then converted by hand to point source geometry.

Program STAR problems were run with various sets of input data differing in the number of energy and angular groups and the upper and lower energy limits. The first problem was based upon the Aronson data and had 8 energy groups over 0.33 to 18.0 Mev and 2 angular groups. Two angular groups is equivalent to a double P_1 treatment of the angular dependence because the number of angular groups refers to the order of Gaussian quadrature used in separate angular integrations over 0 to 1 and -1 to 0 in the direction cosine. This equivalence has been shown

by Gast [19] who cites work showing better results for double P_1 approximations than for ordinary P_3 approximations.

By what now appears to have been a fortuitous event of a very low probability of occurrence, the calculated dose rates for the eight energy group problem were almost exactly the same as those reported by Aronson et al. [17] at distances of more than 30 cm from the source (the same within about 10% which is very good in this work and not separable on the usual semilog plots of the dose rate versus the distance from the source).

Subsequent cases were run with fewer energy groups because the eight energy group problem could not be run to as great a thickness as desired within the five minute limit for ordinary problems at the M. I. T. computation center.

A series of three problems were run to check the effect of changing the number of energy and angular groups. Two and three angular groups with four energy groups over 0.1 to 10.0 Mev and two angular groups with five energy groups over 0.1 to 10.0 Mev based on the Goldstein cross section data were used. The results are presented in Figure 8.

One may conclude that the dose rate is more sensitive to the number of energy groups than to the number of angular groups and that two angular groups are sufficient to reduce the uncertainty due to the angular approximation to less than the uncertainty due to the energy approximation in this problem.

A final water problem was run with six energy groups over 0.33 to 14.1 Mev and two angular groups based on the older cross section data of Aronson et al. A basic change in the preparation of the input

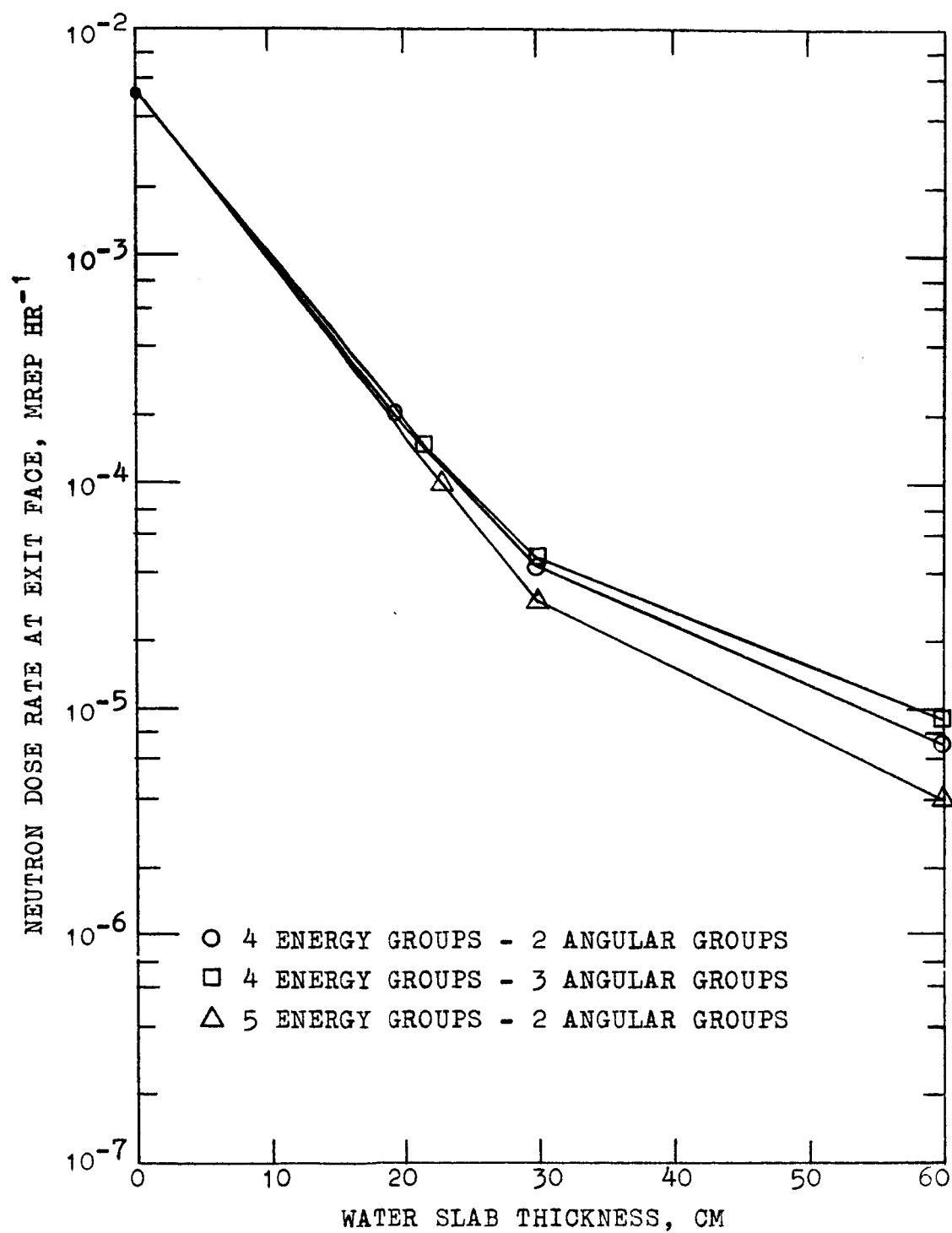


FIGURE 8
DOSE RATE DUE TO A PLANE ISOTROPIC FISSION
SOURCE VERSUS WATER SHIELD THICKNESS

data to program STAR was made in this problem.

The 4, 5, and 8 energy group input data used in the previous water problems was prepared by averaging microscopic cross section data tabulated at 16 or more equally spaced increments in the lethargy variable $u = \ln(E/E_0)$. A unit flux weighting function was used.

The six energy group input data was prepared from microscopic cross sections evaluated at precisely the six incident energies used in the Gaussian quadrature energy integrations. This is a better method of preparing the input data since it is consistent with the numerical integration scheme and avoids the problem of choosing the flux weighting function. Resonances in the cross sections are an obvious problem with this method and some judgment must be exercised in picking representative points for the particular problem at hand or in smoothing out the cross section data. In any case, some approximation with respect to resonances must occur when only a few energy groups are used. In this case the desired upper and lower energy limits were chosen and the cross sections evaluated at the Gaussian quadrature points without approximation because by good fortune the six points were all fairly representative of the overall cross section behavior.

The results of the two angular group, four and six energy group invariant imbedding method problems are compared with other transport theory results in Figures 9 and 10. The solutions designated C9, M1, T5, T5', and T8 were reported by the S. D. of the A. N. S. [14]. The attenuation in plane source geometry is slightly over 10 powers of ten at the maximum thickness of 210 cm of water. Figure 10 has an exponential scale factor applied to remove most of the spatial dependence and

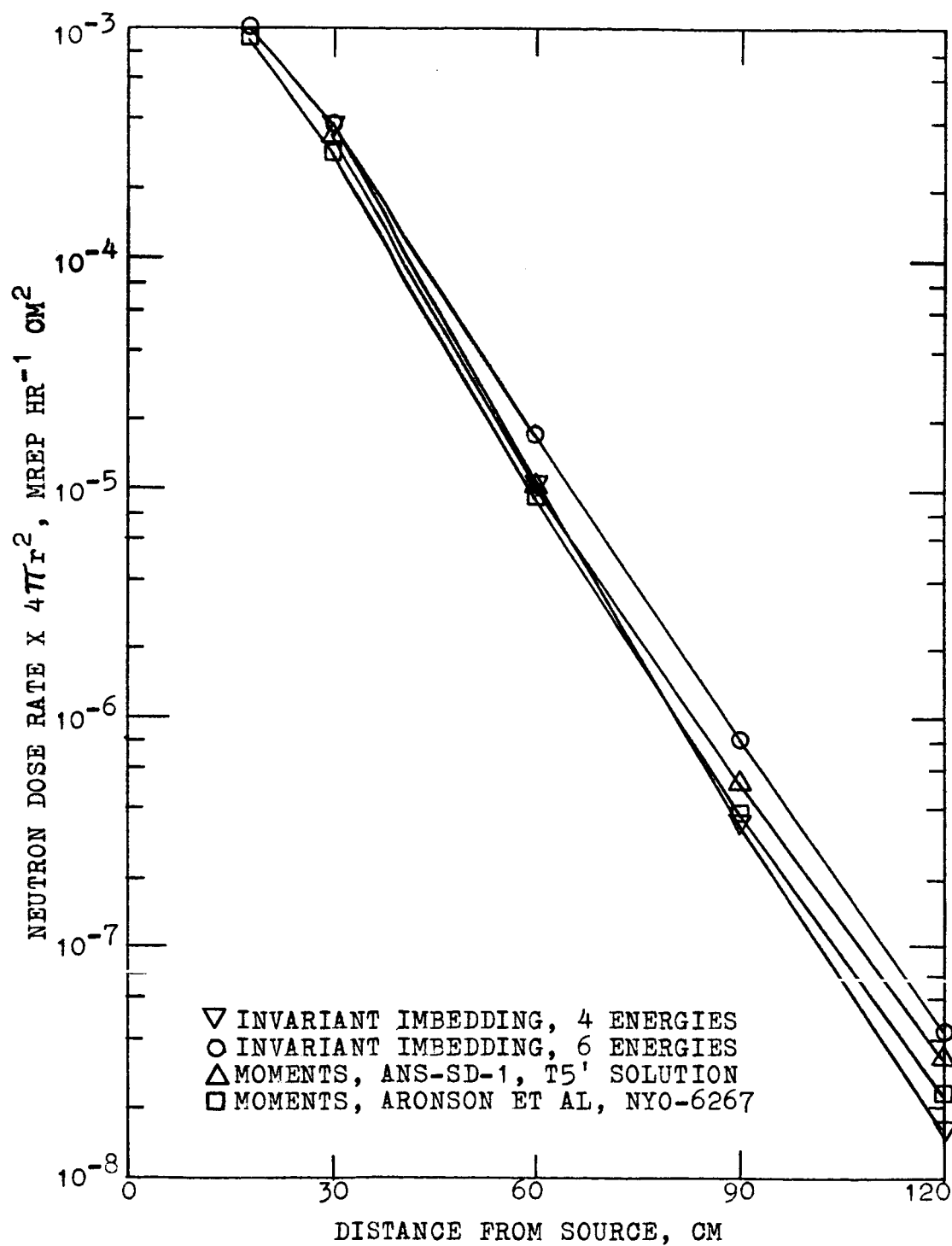


FIGURE 9
DOSE RATE VERSUS DISTANCE FROM A POINT
ISOTROPIC FISSION NEUTRON SOURCE IN WATER

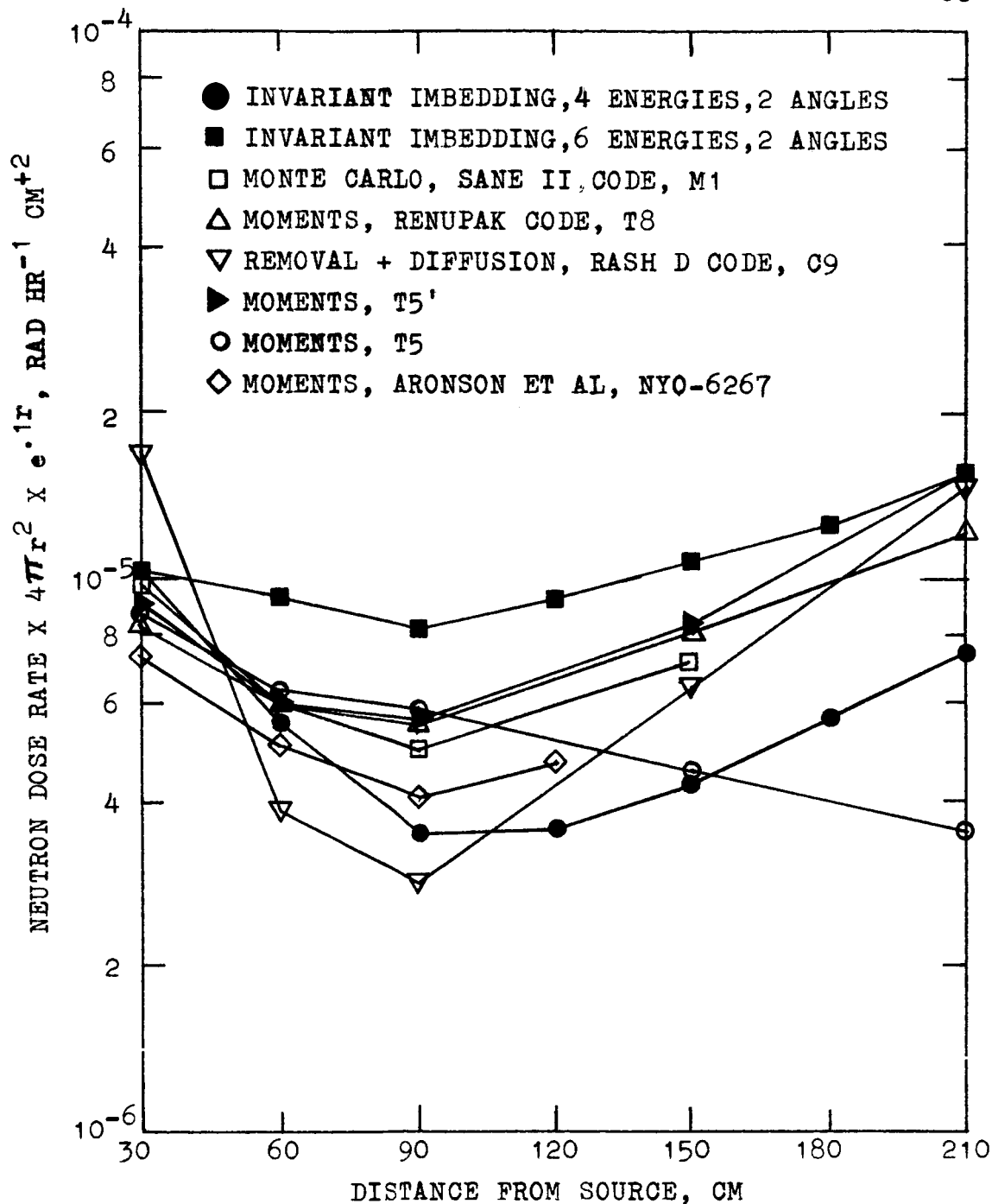


FIGURE 10
 NEUTRON DOSE RATE IN WATER VERSUS DISTANCE
 FROM A POINT ISOTROPIC FISSION SOURCE

accentuate the differences between the various solutions.

The Monte Carlo method solution M1 and the moments method solutions T5' and T8 were judged by the S. D. of the A. N. S. to be the most reliable methods for this problem. The four and six energy group invariant imbedding results bracket these solutions with the six energy group result being closer over most of the range.

The older cross section set of Aronson was used for the six group result whereas the newer cross sections prepared by Goldstein for the A. N. S. problems were used for the four group problem and for the M1, M5' and T8 solutions. The reason for using the older cross section set for the six energy group problem was to try to reproduce as closely as possible the results of Aronson. It was found, however, that in spite of the older cross sections, the calculated result came closer to the later moments method solutions published by the A. N. S.

Neutron energy spectra for the six energy group problem at 10, 90, and 180 cm from the source are presented in Figure 11 as well as a comparison with the spectrum at 90 cm from the moments method results of Aronson [17]. The moments method spectrum was normalized to the same dose rate to facilitate the comparison of the spectral shapes. The agreement in shape is very good, particularly when it is realized that a six energy group computation is being compared with a forty energy group computation.

In summary, it appears that program STAR yields acceptable results compared to other methods for deep penetration calculations in neutron shields made of water. Although not shown in Figures 9 and 10, the A. N. S. solutions include several varieties of the DSN and DTK codes that

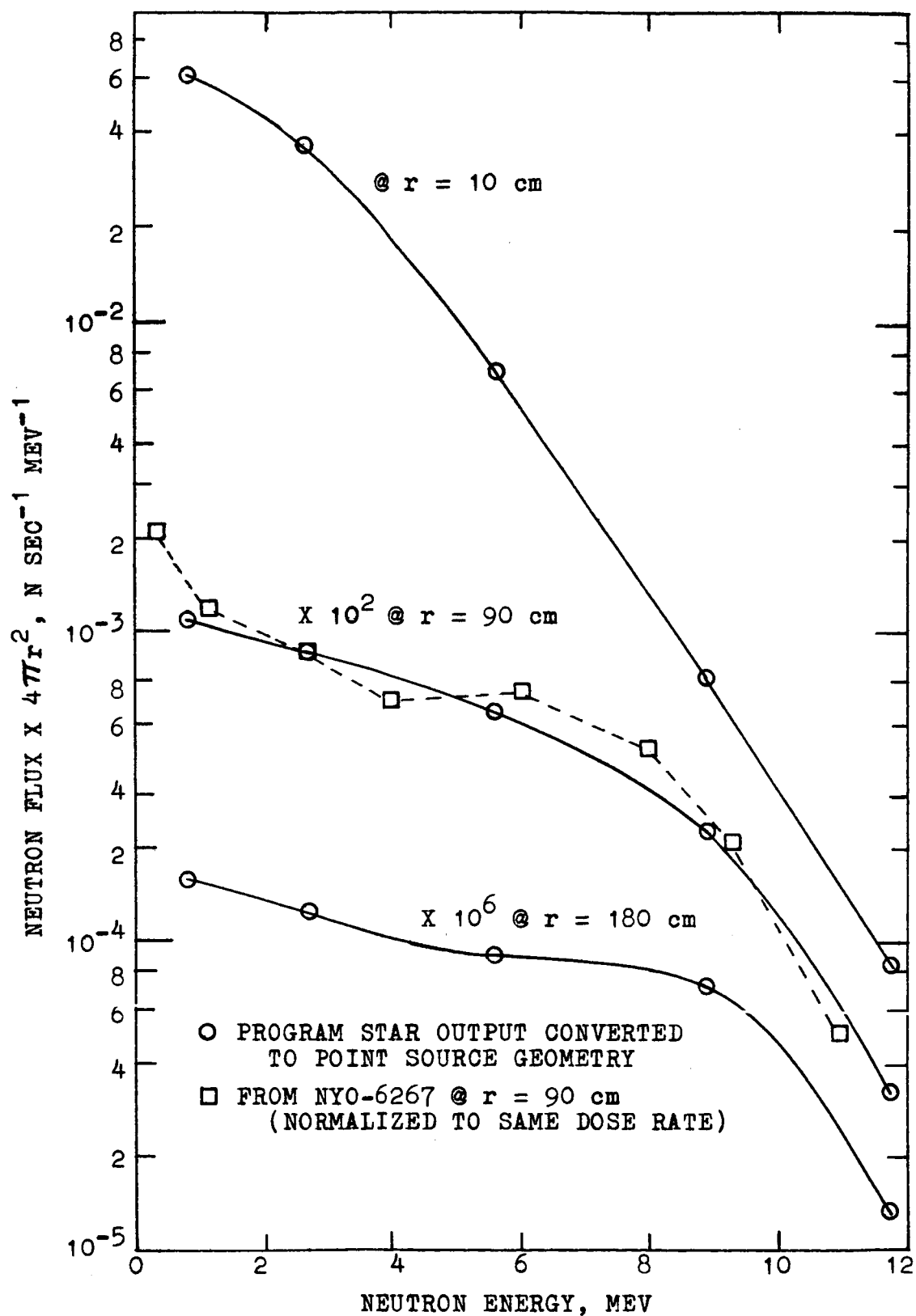


FIGURE 11

NEUTRON FLUX VERSUS ENERGY AND DISTANCE
FROM A POINT ISOTROPIC FISSION SOURCE IN WATER

gave very poor results analogous to diffusion theory (2 to 3 orders of magnitude or more in error at 210 cm thickness). This is apparently due to an inadequate treatment of the anisotropic scattering in water. By contrast the invariant imbedding method STAR does not seem to have difficulty in representing the angular dependence of the cross sections adequately.

Polyenergetic neutrons in a heterogeneous iron/polyethylene shield. The fourth problem is designed to show the ability of the invariant imbedding method to handle heterogeneous problems. A shield composed of 4 inches of iron followed by 6 inches of polyethylene followed by 1 inch of iron is considered. An additional problem was run for a homogeneous polyethylene slab up to 12 inches thick as a reference. A unit isotropic fission neutron source is used.

Two angular groups and both four and five energy groups over 0.1 to 10.0 Mev were used. The cross section data was taken from the set prepared by Goldstein for the A. N. S. shielding problems discussed in connection with the third problem.

The results are presented in Table IV and Figure 12 along with the Monte Carlo method results of Allen et al. [15] converted to a unit isotropic fission source input. A correction in the polyethylene results was necessary because the polyethylene cross sections were prepared for a density of 0.907 gm/cm^3 whereas the results of Allen et al. turned out to be for a polyethylene density of 0.97. The correction was made by increasing the polyethylene thickness by a factor of 1.07, i.e. the 6 inches of polyethylene was increased to 6.43 inches and the 12 inches of polyethylene was increased to 12.8 inches.

TABLE IV

NEUTRON DOSE TRANSMISSION FACTORS FOR A UNIT ISOTROPIC
FISSION SOURCE INCIDENT UPON IRON/POLYETHYLENE SHIELDS

Shield	Dose Transmission Factor		
	4 Group STAR	5 Group STAR	Monte Carlo
12" Polyethylene	0.0018	0.0015	0.0014
4" Iron/6" Polyethylene/ 1" Iron	0.0096	0.0075	0.0069

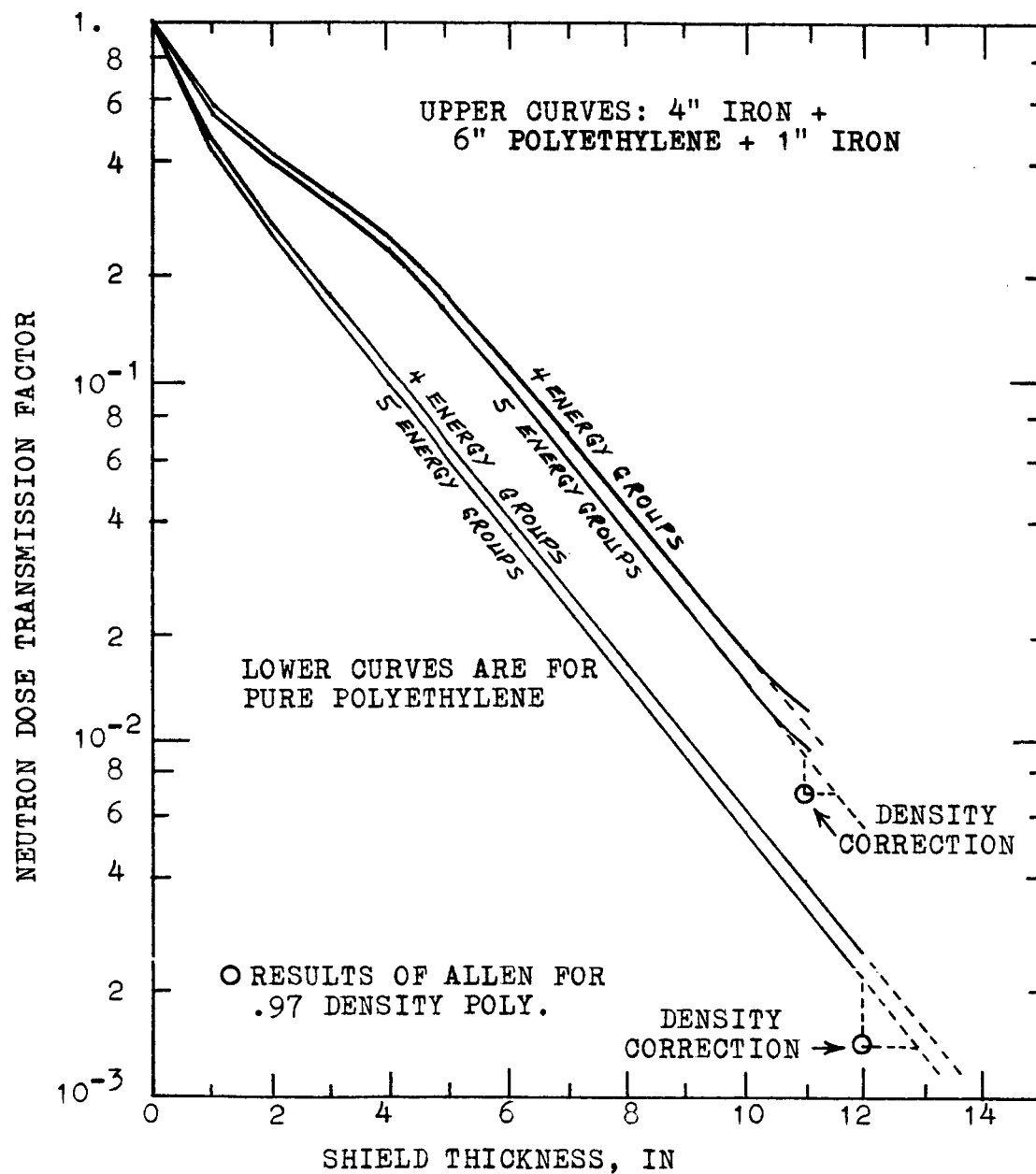


FIGURE 12
NEUTRON DOSE TRANSMISSION FACTOR FOR A UNIT ISOTROPIC
FISSION SOURCE INCIDENT UPON IRON/POLYETHYLENE SHIELDS

The five energy group results compare better than the four energy group results as one would expect. The agreement is within 8% for the five energy group problem. This is well within the accuracy of the conversion of the monoenergetic Monte Carlo method results of Allen et al. to the fission source input.

Discussion. The results of this chapter indicate that the most useful applications of the invariant imbedding method will probably be in problems in which the moments method does not apply because of heterogeneity and in which the attenuation is large enough to make the Monte Carlo method unattractive on account of excessive computing time and in which the scattering is sufficiently anisotropic to make the application of the usual varieties of DSN or DTK type transport theory codes suspect.

The computing time required for the various problems is presented in Table V. The three problems run on 12/27/65 were included to illustrate the variation in computing time with the number of energy and angle groups even though the program was not as fast as the final version (note that the error criterion is larger for these problems).

The variable step size feature of program STAR works very well. The variation of the reflection and transmission step sizes with shield thickness for the five energy group calculation in the three region iron/polyethylene shield is shown in Figure 13. The step size gradually increases in a region and is automatically adjusted to a smaller size at the start of the next region. Note that the transient change is much larger in going from the iron into the polyethylene than vice versa as

TABLE V
COMPUTING TIME REQUIRED BY INVARIANT
IMBEDDING PROBLEMS

PROBLEM NUMBER	MAXIMUM THICKNESS	NUMBER OF ENERGY GROUPS	NUMBER OF ANGULAR GROUPS	ERROR CRITERION	MAXIMUM STEP	MAXIMUM SIZE	DATE RUN	TIME IN MINUTES
					<u>T</u>	<u>R</u>		
I	210.	1	1	1.0E-05	1.	5.	1/14/66	0.62
II	6.	1	7	1.0E-03	.0254	.125	1/15/66	1.68
III	210.	6	2	1.0E-02	.465	2.325	1/16/66	4.93
	210.	4	3	1.0E-01	.44	100.	12/27/65	4.19
	210.	5	2	1.0E-01	.44	100.	12/27/65	2.48
	210.	4	2	1.0E-01	.44	100.	12/27/65	1.59
IV	27.94	4	2	1.0E-02	.68	3.40	1/16/66	1.52
	27.94	5	2	1.0E-02	.68	3.40	1/17/66	1.75

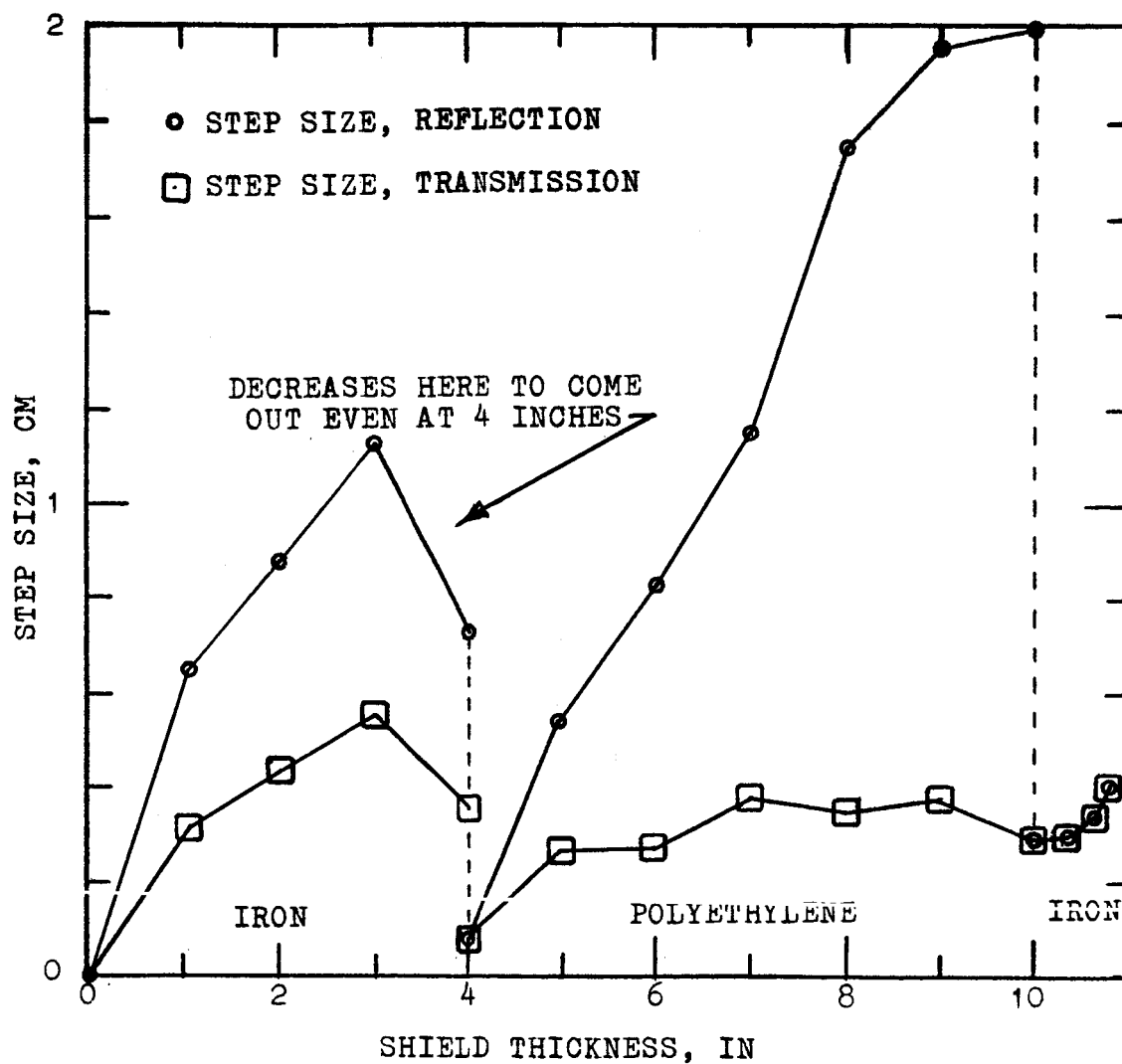


FIGURE 13
STEP SIZE VARIATION IN THE FIVE ENERGY GROUP PROBLEM IV

one would expect since, because of its hydrogen content, the polyethylene is less transparent to neutrons than iron.

The effect on the required computer time of the variable step size and the setting of the reflection to a constant value when the derivative of the reflection with respect to shield thickness becomes less than 0.001 is dramatic. In the six energy group water problem run on 1/16/66, the first 12.6 cm required 1.26 min. or 0.100 min/cm. At this point the reflection was set equal to a constant value and the next 17.4 cm required 0.24 min for a rate of 0.0138 min/cm which is over seven times faster than the initial rate. The final rate for this problem was 0.0131 min/cm for thicknesses of over 30 cm (plus 4.4 sec for each printed point).

The 1.7 min required for the seven angular group monoenergetic problem run on 1/15/66 compares quite favorably with the approximately 10 min per five angular group monoenergetic problem reported by Beissner [4]. An additional 0.5 min would have been required to continue to the same 10 mfp thickness used by Beissner but experiments with a variable number of angular groups in the monoenergetic problem have indicated that program STAR is about 3.5 times faster for five angular groups as compared to seven angular groups. This means that about 0.6 min would be required for the program STAR problem comparable to the 10 min problem of Beissner.

After taking into account the difference in speed between the computers used (IBM-7094 versus IBM-7090), it is clear that program STAR is considerably faster even for this thin shield problem in which the high speed transmission only calculation of program STAR was not used because the reflection does not closely approach its asymptotic

value until nearly the end of the computation.

Noting that the number of operations required to evaluate the nonlinear double sum term increases as the fourth power of the product of the number of energy groups and the number of angular groups, one may estimate (not stated by Beissner) that the energy dependent computations with six energy groups and 3 angular groups performed by Beissner [6] must have required several hours of computer time. This may explain why no further energy dependent results have been reported by Beissner.

CHAPTER V

CONCLUSIONS AND SUGGESTIONS FOR FURTHER WORK

In plane geometry shielding problems in which the shield is very heterogeneous, i.e., composed of many layers of differing materials, the invariant imbedding method seems to offer clear cut advantages over other methods because the computer fast memory requirement is not affected by the degree of heterogeneity of the problem. In addition, there is no need to specify a mesh spacing for the spatial variable and the memory requirement is not a function of the number of spatial points considered.

In its present form, the invariant imbedding method also seems to be the method of choice in plane geometry shielding problems in which the following three conditions are satisfied: 1) the shield is heterogeneous so that the moments method does not apply, 2) the attenuation is sufficiently large so that the Monte Carlo method requires an excessive amount of computing time and, 3) the scattering is sufficiently anisotropic so that the application of the usual varieties of the SNG or DSN type transport theory codes is suspect.

Double Gaussian quadrature at a total of $2n$ points where n is two or three was shown to be adequate to approximate the angular dependence even in the water penetration problem in which DSN type codes incorporating a linear anisotropic scattering correction failed badly. The success of the low order angular approximations is attributed in part to the separation of the transmitted flux into scattered and unscattered components and in part to the use of the double Gaussian quadrature.

The use of Gaussian quadrature to approximate the energy dependence worked well and reasonable results were obtained with four

to six energy groups in the fast neutron region. The problem of how best to approximate the energy dependence cannot, however, be regarded as settled in the same sense that it appears that double Gaussian quadrature is a clearly superior method of treating the angular dependence. One serious shortcoming of the present method is that thermal and epithermal neutrons are ignored. For this reason it would probably be better to rewrite the basic reflection and transmission equations in terms of the lethargy variable and to approximate the lethargy dependence.

A very simple numerical approximation which is exact for an exponential function was found to work very well for the numerical solution of the reflection and transmission equations. The following features were found useful in accelerating the solution of the plane geometry reflection and transmission equations: 1) a variable step size which is automatically adjusted to give a desired value for the estimated relative truncation error per step regardless of the material properties of the region, 2) a different step size for the reflection and transmission calculations allowing the more difficult reflection calculation to be performed less often and, 3) the termination of the reflection calculation when the reflection closely approaches its asymptotic value.

It was found necessary to limit the maximum allowable step size in the transmission calculation on account of numerical instability at large step sizes. This places a limit on the speed of the solution since in the outer portions of a thick shield layer, the step size in the transmission equation solution is limited by the numerical stability limit to step sizes much smaller than would otherwise be allowed by

stepwise error considerations.

Fortunately, the transmission equation solution when the reflection is assumed to have attained its asymptotic value is so much faster than the combined reflection and transmission calculations at the beginning of a shield layer that this limit has not been too restrictive in practice. However, it would be much better if a method of avoiding the numerical instability could be devised which would still allow large step sizes with small error and further work in this area is suggested.

Beissner [4] suggested that in some cases in which forward scatter is large compared to backward scatter, one might be able to neglect the double sum terms in the reflection and transmission equations (3.4) and (3.11). This does not seem to be a very good approximation in practical circumstances over most of the range of the reflection and transmission variables. There is, however, a real incentive to investigate some such scheme because whenever the double sum terms can be neglected, the number of operations required to evaluate the right-hand-sides of the differential equations drops from a fourth power to a third power dependence upon the number of particle states and most of the computer time required for these problems is consumed in these evaluations.

The double sum terms can certainly be neglected at the first step and the question is to how to set up some criterion for deciding for how many more steps they can be neglected. This could turn out to be significant since the step size is smallest near the origin and a substantial fraction of the computer time required for any given problem is consumed in advancing the solution in the region near the origin.

The combination of some way to eliminate unnecessary evaluations of the double sum terms coupled with a numerical solution of the transmission equation with a less restrictive stability limit could potentially make the invariant imbedding method the method of choice for a very wide range of plane geometry shielding problems.

Finally, there seems to be little incentive to apply the invariant imbedding method to criticality calculations in plane geometry. There are easier methods of obtaining criticality estimates in plane geometry without becoming so involved in the details of the flux distributions.

There is a possibility, however, that the invariant imbedding method may have a useful application to criticality calculations for right circular cylindrical shapes. Because this case is of great practical interest the idea will be discussed in some detail. Basically, one imagines that a cylinder is built up from a series of thin discs in the same way that a right circular cylinder may be built up by stacking coins and considers the reflection of neutrons from one end of the cylinder as the height of the cylinder varies. A very complicated reflection equation may be derived by following the approach given by Chandrasekhar [20]. For purposes of illustration, a reflection equation is given for the greatly simplified case in which it is assumed that the properties of the cylinder vary only in the axial direction, that the reflection is not dependent upon the azimuthal position in the cylinder, and that the neutrons all have a common velocity.

Let z and ρ represent the axial and radial position, respectively, and let μ represent the cosine of the angle between the neutron direction and the $+z$ direction. The reflection of a unit pencil of neutrons

incident at the center of the end surface of a right circular cylinder of radius R_0 and height z is given by the equation

$$\begin{aligned} \frac{\partial}{\partial z} R(z, 0; -1, 1) = & \sigma(z)g(z; -1, 1) - 2\sigma(z)R(z, 0; -1, 1) + \left[\sigma(z) \right. \\ & \left. \int_0^1 d\mu' g(z; \mu', 1) R(z, 0; -1, \mu') \right] + \left[\sigma(z) \int_0^1 \frac{d\mu''}{\mu''} R(z, 0; -\mu'', 1) \right. \\ & \left. g(z; -1, -\mu'') \right] + 2\pi \left[\sigma(z) \int_0^1 \frac{d\mu''}{\mu''} \int_0^{R_0} \rho' d\rho' \right. \\ & \left. \int_0^1 d\mu' R(z, \rho'; -\mu'', 1) g(z, \mu', -\mu'') R(z, \mu'; -1, \mu') \right] \end{aligned} \quad (5.1)$$

with the familiar initial condition

$$R(0, \rho; \mu', \mu) = 0, \quad (5.2)$$

that is, the reflection is zero at zero thickness (cylinder height in this case) for all radii and direction cosines.

Note that the reflection equation is similar in many ways to the plane geometry reflection equation except that it is now a partial differential equation with a triple integral for the last term instead of the double integral in the plane geometry case, the additional integration being over the radial coordinate.

For criticality one desires to find out the value of z for which the reflection diverges toward infinity. The value of the reflection itself is not important and any convenient type of incident source may be used to obtain an equation for the reflection. The relatively simple form of the above equation for the reflection is partly a consequence of a judicious choice of the incident source so that several terms in the more general reflection equation vanish. This simplified equation shows clearly, however, the general nature of invariant

imbedding equation in this cylindrical geometry case. It is hoped that this discussion will stimulate further investigation to see if a practical procedure can be developed applying the invariant imbedding method in this special case of cylindrical geometry.

In summary, the invariant imbedding method has been shown to yield useful results in a practical length of time in certain cases of practical interest in neutron shielding. The areas in which further work has been suggested include: 1) transformation to the lethargy variable, 2) investigation of more stable numerical solution techniques for the transmission equation, 3) elimination of unnecessary evaluations of the nonlinear term, and 4) the possible application of the invariant imbedding method to the calculation of the critical height for a right-circular cylinder.

APPENDIX A

INPUT DATA PREPARATION

Introduction

The numerical solution of the plane geometry reflection and transmission equations requires the following input data: 1) the abscissas and weights for the integrations over energy, 2) the abscissas and weights for the integrations over the particle direction cosines, 3) the average value of the total macroscopic cross section for each energy group, 4) the average value of the mean number of secondaries per collision for each energy group, and 5) the probability of transfer from one particle state to another particle state as a result of a collision.

The following sections are restricted to the preparation of input data for neutron transport problems only, but similar procedures could be used to generate input data for gamma ray transport problems.

The state-to-state transfer probability matrix contains all of the information concerning the angular dependence of the scattering processes in the scattering medium. At the energies of interest in nuclear reactor shielding problems, the interactions of neutron with nuclei which must be considered are : 1) elastic scattering, 2) inelastic scattering, 3) $n, 2n$ reactions, and 4) fission reactions. Only the elastic scattering process contributes an anisotropic component to the state-to-state transfer probability since the other processes may be assumed to result in an isotropic angular distribution of scattered neutrons in the laboratory coordinate system.

The fission process is included in this section only for generality. In a shield, fissionable material will not ordinarily be present. If there is no fissionable material, neutrons can not increase in energy after entering the shield, and those elements of the state-to-state transfer probability matrix for which the neutron energy would

increase are zero and do not have to be calculated.

The cross section data preparation computer program (program CSDP) listed in Appendix D solves the equations of this chapter for a maximum of 5 nuclides tabulated at a maximum of 100 energy points and provides punched output in a suitable format for input to the computer program (program STAR) for the solution of the plane geometry reflection and transmission equations listed in Appendix C.

Abscissas and Weights for Numerical Integrations

Any desired numerical integration formula may be used to compute the abscissas and weights that are required for the numerical solution of the reflection and transmission equations. It is not necessary to use the same formula for the integrations over energy as for the integrations over particle direction cosines.

In this investigation, Gaussian quadrature was used for both integrations. The abscissas and weights for the energy integrations were obtained from

$$E_k = [(EH_n - EL_1)/2] (1 + ETA_{k,n}) + EL_1 \quad (1)$$

$$WE_k = [(EH_n - EL_1)/2] W_{k,n} \quad (2)$$

where $ETA_{k,n}$ and $W_{k,n}$ are the abscissas and weights tabulated by Lowan, Davids, and Levenson [22] for Gaussian quadrature at n points in the interval $(-1,1)$, EL_1 is the lower limit of the lowest energy group, and EH_n is the upper limit of the highest energy group.

Similarly, the abscissas and weights for integrations over particle direction cosines were obtained from

$$MU_j = (1 + ETA_{j,n})/2 \quad (3)$$

$$WMU_j = W_{j,n}/2 \quad (4)$$

Total Cross Section

The macroscopic total cross section for each energy group, TCS_k , was obtained from

$$TCS_k = \frac{\sum_{i=1}^{NN} AD_i \int_{EL_k}^{EH_k} \phi(E) \sigma_{t,i}(E) dE}{\int_{EL_k}^{EH_k} \phi(E) dE} \quad (5)$$

where AD_i is the atom density of the i th nuclide, NN is the number of nuclides, $\phi(E)$ is the neutron flux as a function of energy, and $\sigma_{t,i}(E)$ is the microscopic total cross section of the i th nuclide as a function of energy.

The trapezoidal rule was used to evaluate (5) because the energy points at which $\sigma_{t,i}(E)$ is tabulated are not always uniformly spaced and cannot be chosen in advance.

Mean Number of Secondaries per Collision

The mean number of secondaries per collision for the i th nuclide as a function of energy, $c_i(E)$, is

$$c_i(E) = \frac{\nu_i(E) \sigma_{f,i}(E) + \sigma_{s,i}(E) + 2 \sigma_{n2n,i}(E)}{\sigma_{t,i}(E)} \quad (6)$$

and the mean number of secondaries per collision for the k th energy group, C_k , is

$$C_k = \frac{\sum_{i=1}^{NN} AD_i \int_{EL_k}^{EH_k} \phi(E) c_i(E) dE}{AD_t \int_{EL_k}^{EH_k} \phi(E) dE} \quad (7)$$

where $\nu_1(E)$ is the mean number of neutrons per fission for the i th nuclide as a function of energy, $\sigma_{f,i}(E)$ is the microscopic fission cross section, $\sigma_{s,i}(E)$ is the microscopic scattering cross section (includes both elastic and inelastic scattering), $\sigma_{n2n,i}(E)$ is the microscopic $n,2n$ reaction cross section, and AD_t is the total atom density.

The trapezoidal rule was used to evaluate (7).

State-to-State Transfer Probability

Let $P(E_k, E_m; \Omega_j, \Omega_l)$ be the probability of transfer of a neutron from energy E_k and direction Ω_j into unit energy about E_m and into unit solid angle about Ω_l as a result of a collision with the normalization

$$\int_0^\infty dE_m \int_{\text{all } \Omega} d\Omega_l P(E_k, E_m; \Omega_j, \Omega_l) = 1. \quad (8)$$

The sum of the fission, inelastic, and $n,2n$ contributions to the transfer probability is

$$P_{f+in+n2n}(E_k, E_m; \Omega_j, \Omega_l) = \frac{1}{4\pi} \sum_{i=1}^{NN} \frac{AD_i}{AD_t} \left[\nu_1(E_k) \sigma_{f,i}(E_k) g_{f,i}(E_k, E_m) + \sigma_{in,i}(E_k) g_{in,i}(E_k, E_m) + \sigma_{n2n,i}(E_k) g_{n2n,i}(E_k, E_m) \right] / [c_1(E_k) \sigma_{t,i}(E_k)] \quad (9)$$

where $g_{f,i}(E_k, E_m)$ is the energy spectrum of neutrons emitted in a fission reaction caused by a neutron of energy E_k incident upon the i th type of nucleus, $g_{in,i}(E_k, E_m)$ is the energy spectrum of inelastically scattered neutrons, and $g_{n2n,i}(E_k, E_m)$ is the energy spectrum of neutrons emitted in

the n,2n reaction.

The various energy spectra are subject to the normalization conditions

$$\int_0^{\infty} g_{f,i}(E_k, E_m) dE_m = 1 \quad (10)$$

$$\int_0^{\infty} g_{in,i}(E_k, E_m) dE_m = 1 \quad (11)$$

$$\int_0^{\infty} g_{n2n,i}(E_k, E_m) dE_m = 2 \quad , \quad (12)$$

that is, the fission and inelastic energy spectra are normalized to unity and the n,2n reaction energy spectrum is normalized to two in order to make maximum use of existing data.

Let the differential elastic scattering cross section in the center-of-mass (C.M.) coordinate system be represented by an expansion in a finite series of Legendre polynomials of the form

$$\sigma_{e,i}(E_k, \mu_c) = \frac{\sigma_{e,i}(E_k)}{4\pi} \left[1 + \sum_{l=1}^N (2l+1) F_{l,i}(E_k) P_l(\mu_c) \right] \quad (13)$$

where $\theta_c = \cos^{-1} \mu_c$ is the deflection angle in the C.M. system, the $F_{l,i}(E_k)$ are coefficients tabulated as functions of energy for each nuclide, the $P_l(\mu_c)$ are Legendre polynomials of order l , and

$$\sigma_{e,i}(E_k) = \int_0^{2\pi} d\phi \int_{-1}^1 d\mu_c \sigma_{e,i}(E_k, \mu_c) \quad . \quad (14)$$

If $\theta = \cos^{-1} \mu$ is the deflection angle in the laboratory (L.) coordinate system, $d\Omega = d\mu d\phi$ is a differential element of solid angle in the L. system, and $d\Omega_c = d\mu_c d\phi$ is an element of solid angle in the C.M. system, then

$$\sigma_{e,i}(E_k, \mu) d\mu d\phi = \sigma_{e,i}(E_k, \mu_c) d\mu_c d\phi \quad (15)$$

or

$$\sigma_{e,i}(E_k, \mu) = \sigma_{e,i}(E_k, \mu_c) d\mu_c / d\mu \quad (16)$$

The elastic scatter contribution to the transfer probability is

$$P_e(E_k, E_m; \Omega_j, \Omega_1) = \sum_{i=1}^{NN} \frac{AD_i}{AD_t c_1(E_k)} \frac{\sigma_{e,i}(E_k, \mu_c)}{\sigma_{t,i}(E_k)} \frac{d\mu_c}{d\mu} \delta \left\{ E_m - E_k \left[\frac{\sqrt{A_1^2 - 1 + \mu^2} + \mu}{A_1 + 1} \right]^2 \right\} \quad (17)$$

where

$$\mu = \Omega_j \cdot \Omega_1 = \mu_j \mu_1 + \sqrt{1 - \mu_j^2} \sqrt{1 - \mu_1^2} \cos(\phi_1 - \phi_j) \quad (18)$$

$$\mu_c = \left[\mu (\sqrt{A_1^2 - 1 + \mu^2} + \mu) - 1 \right] / A_1 \quad (19)$$

and where A_1 is the mass number of the target nucleus and the Dirac delta function is necessary to conserve energy (cf. Weinberg and Wigner [23]). Differentiation of (19) gives

$$\frac{d\mu_c}{d\mu} = \frac{(\sqrt{A_1^2 - 1 + \mu^2} + \mu)^2}{A_1 \sqrt{A_1^2 - 1 + \mu^2}} \quad (20)$$

The transfer probability for azimuthally symmetric scattering (the usual case) is obtained by integrating (9) and (17) over all possible values of ϕ_1 . Defining $\phi = \phi_j - \phi_1$ and using the symmetry of $\cos\phi$ in $(0, 2\pi)$, one obtains

$$P(E_k, E_m; \mu_j, \mu_1) = \sum_{i=1}^{NN} \frac{AD_i}{AD_t} \left\{ \begin{aligned} & \frac{1}{2} \left[\nu_i(E_k) \sigma_{f,i}(E_k) g_{f,i}(E_k, E_m) + \sigma_{in,i}(E_k) g_{in,i}(E_k, E_m) + \right. \\ & \left. \sigma_{n2n,i}(E_k) g_{n2n,i}(E_k, E_m) \right] + \end{aligned} \right. \quad (21)$$

$$2 \int_0^\pi \sigma_{e,i}(E_k, \mu_c) \frac{d\mu_c}{d\mu} \delta \left[\begin{matrix} E_m - E_k \\ \left[c_i(E_k) \sigma_{t,i}(E_k) \right] \end{matrix} \left(\frac{\sqrt{A_1^2 - 1 + \mu^2} + \mu}{A_1 + 1} \right)^2 \right] d\phi /$$

where μ , μ_c , and $d\mu_c/d\mu$ are all functions of ϕ .

Define the state-to-state transfer probability, $TP(SE_{1,m}; SI_{j,k})$, as the probability that a neutron will be transferred from incident state $SI_{j,k}$ (incident direction cosine in direction cosine group j and incident energy in energy group k) into a differential direction cosine range and into a differential energy range in exit state $SE_{1,m}$ (exit direction cosine in direction cosine group 1 and exit energy in energy group m). The state-to-state transfer probability is obtained by averaging (21) over the incident and exit directions and energies in the following manner

$$TP(SE_{1,m}; SI_{j,k}) = \quad (22)$$

$$\frac{\int_{EL_k}^{EH_k} dE_1 \int_{MUL_j}^{MUH_j} dMU_1 \int_{MUL_1}^{MUH_1} dMU_2 \int_{EL_m}^{EH_m} dE_2 \phi(E_1, MU_1) P(E_1, E_2; MU_1, MU_2)}{(MUH_1 - MUL_1) (EH_m - EL_m) \int_{EL_k}^{EH_k} dE_1 \int_{MUL_j}^{MUH_j} dMU_1 \phi(E_1, MU_1)}$$

where $\phi(E_1, MU_1)$ is a weighting function that would be the energy and direction dependent neutron flux, if that flux were known.

The fission, inelastic, and $n, 2n$ terms in (21) do not depend on direction. The contribution to the state-to-state transfer probability from these processes is

$$TP_{f+1n+n2n}(SE_{l,m};SI_{j,k}) = \frac{1}{2} \sum_{i=1}^{NN} \frac{AD_i}{AD_t} \left\{ \frac{\int_{EL_k}^{EH_k} dE_1 \int_{EL_m}^{EH_m} dE_2 \phi(E_1) P_{f+1n+n2n,1}(E_1, E_2)}{(EH_m - EL_m) \int_{EL_k}^{EH_m} dE_1 \phi(E_1)} \right\} \quad (23)$$

where $\phi(E_1, MU_1)$ has been assumed to depend on E_1 only and where

$$P_{f+1n+n2n,1}(E_1, E_2) = \left[\nu_1(E_1) \sigma_{f,1}(E_1) g_{f,1}(E_1, E_2) + \sigma_{1n,1}(E_1) g_{1n,1}(E_1, E_2) + \sigma_{n2n,1}(E_1) g_{n2n,1}(E_1, E_2) \right] / \left[c_1(E_1) \sigma_{t,1}(E_1) \right] \quad (24)$$

The contribution to the state-to-state transfer probability from the elastic scattering process is

$$TP_{e,1}(SE_{l,m};SI_{j,k}) = \sum_{i=1}^{NN} \frac{AD_i}{AD_t} \left\{ \frac{\int_{EL_k}^{EH_k} dE_1 \int_{MUL_j}^{MUH_j} dMU_1 \phi(E_1, MU_1) \int_{MUL_1}^{MUH_1} dMU_2 \int_{EL_m}^{EH_m} dE_2 \int_0^{2\pi} d\phi P_{e,1}}{(MUH_1 - MUL_1)(EH_m - EL_m) \int_{EL_k}^{EH_k} dE_1 \int_{MUL_j}^{MUH_j} dMU_1 \phi(E_1, MU_1)} \right\} \quad (25)$$

where

$$P_{e,1} = P_{e,1}(E_1, E_2; MU_1, MU_2, PHI) = \quad (26)$$

$$\frac{2 \sigma_{e,1}(E_1, MUC) \frac{dMUC}{dMU} \delta \left[E_2 - E_1 \left(\frac{\sqrt{A_1^2 - 1 + MU^2}}{A_1 + 1} + MU \right)^2 \right]}{c_1(E_1) \sigma_{t,1}(E_1)}$$

$$MU = (MU_1)(MU_2) + \sqrt{1 - MU_1^2} \sqrt{1 - MU_2^2} \cos(PHI) \quad (27)$$

$$MUC = \left[MU (\sqrt{A_1^2 - 1 + MU^2} + MU) - 1 \right] / A_1 \quad (28)$$

$$\frac{dMUC}{dMU} = \frac{(\sqrt{A_1^2 - 1 + MU^2} + MU)^2}{A_1 \sqrt{A_1^2 - 1 + MU^2}}, \quad (29)$$

and $\sigma_{e,1}(E_1, MUC)$ is given by (13) with E_k and μ_c replaced by E_1 and MUC , respectively.

One integration in (25) may be carried out analytically by interchanging the order of the integrations over E_2 and PHI and using the properties of the Dirac delta function in (26). The result is

$$\int_{EL_m}^{EH_m} dE_2 \int_0^\pi dPHI P_{e,1} = \begin{cases} 0 & \text{when } E' \text{ not in } (EL_m, EH_m) \\ 2 \int_0^\pi \frac{\sigma_{e,1}(E_1, MUC) \frac{dMUC}{dMU}}{c_1(E_1) \sigma_{t,1}(E_1)} dPHI & \text{Otherwise} \end{cases} \quad (30)$$

where

$$E' = E_1 \left[\frac{\sqrt{A_1^2 - 1 + MU^2}}{A_1 + 1} + MU \right]^2. \quad (31)$$

The remaining integrals over the incident energy, E_1 , the incident direction cosine, MU_1 , the exit direction cosine,

MU_2 , and the azimuthal angle, Φ , constitute the four-fold integration required for each nuclide for each element of the elastic scatter contribution to the state-to-state transfer probability matrix.

The trapezoidal rule was used for the integration over E_1 in (23) and (25) and for the integration over E_2 in (23). Gaussian quadrature was used for the integrations over MU_1 , MU_2 , and Φ in (23).

Discussion

The equations of the previous section have special forms for hydrogen. For any nuclide such as hydrogen for which elastic scattering may be assumed to be isotropic in the center-of-mass system, (13) becomes simply

$$\sigma_{e,1}(E_1, MUC) = \frac{\sigma_{e,1}(E_1)}{4\pi} \quad (32)$$

Setting A_1 to one in (28), (29), and (31) yields the special forms

$$MUC = \begin{cases} -1 & \text{when } MU \leq 0 \\ 2(MU)^2 - 1 & \text{when } MU > 0 \end{cases} \quad (33)$$

$$\frac{dMUC}{dMU} = \begin{cases} 0 & \text{when } MU \leq 0 \\ 4(MU) & \text{when } MU > 0 \end{cases} \quad (34)$$

$$E' = \begin{cases} 0 & \text{when } MU \leq 0 \\ E_1(MU)^2 & \text{when } MU > 0 \end{cases} \quad (35)$$

where MU is given by (27) as before.

A useful check of the state-to-state transfer probability matrix may be based on the normalization condition (8) in the discrete form

$$\sum_{SE=1}^{NS} [TP(SE;SI) + TP(SE+NS;SI)] WMU(SE)WE(SE) = 1 \quad (36)$$

where NS is the number of particle states (number of energy groups times number of angular groups in (0,1)) and where the term TP(SE+NS;SI) is necessary to include all possible exit states. By definition, states 1 to NS include all energy groups and all negative direction cosines and states NS+1 to 2(NS) include all energy groups and all positive direction cosines. In this scheme, the particle direction is reversed without change in energy group by adding or subtracting NS from the state index.

A sum based upon the left-hand-side of (36), plus an additional component when the lowest energy limit, EL_1 , is greater than zero and energy transfer below this energy is possible, is computed and printed under the heading SUMSCS(1)...SUMSCS(NS) as a check on the values of the transfer probability matrix. This sum should be unity and, in practice, was found to be within 0.5% of unity for hydrogen (the worst case) when 4 point Gaussian quadrature was used for the integrations over MU_1 and MU_2 and 8 point Gaussian quadrature used for the integration over PHI in (25).

The check sum is then used to normalize the values of the transfer probability matrix exactly to unity and recomputed strictly according to (36) without correction for the lower energy limit to show the fraction of neutrons being transferred below the lowest energy group.

The weighting function $\phi(E_1, MU_1)$ in equation (25) was assumed to be a function of E_1 only.

The fraction of fission spectrum neutrons emitted in energy group k, denoted by $FISS_k$, is also calculated and punched out for use in program STAR.

APPENDIX B

OUTPUT DATA PROCESSING

Introduction

The relations between the reflection and transmission variables used in this work and other variables such as neutron angular distribution functions, vector currents, scalar fluxes, and dose commonly used in neutron transport theory are summarized in this chapter.

The relation between point and plane sources is also discussed.

The reflection and transmission variables are defined in the same manner as Chandrasekhar's S and T functions [2]. This reflection must be divided by four times the exit direction cosine in order to correspond to the reflection values tabulated by Bellman, Kalaba, and Prestrud [13].

The transmission variable used in this work includes only diffusely transmitted neutrons, i.e., neutrons that have undergone at least one interaction with the medium through which the neutrons have passed. The uncollided component of the transmission in plane geometry is

$$T_u(SE_{1,m}; SI_{j,k}) = \begin{cases} 0 & \text{when } SE \neq SI \\ \frac{2 MU_j}{WMU_j WE_k} \left[\exp -\frac{1}{MU_j} \int_0^x TCS_k dx' \right] & \end{cases} \quad (1)$$

where $SI_{j,k}$ is the incident neutron state index for a neutron in direction cosine group j and energy group k

($SI_{j,k} = \text{NEREG}(j-1) + k$), $SE_{1,m}$ is the exit neutron state index for a neutron in direction cosine group 1 and energy group m ($SE_{1,m} = \text{NEREG}(1-1) + m$), NEREG is the number of energy groups, MU_j is the value of the direction cosine

assigned to the j th group, WMU_j is the width of the j th direction cosine group, WE_k is the width of the k th energy group, TCS_k is the total macroscopic cross section in the k th energy group, and X is the slab thickness.

The total transmission, T_t , is obtained by adding the corresponding elements of the diffuse transmission, T , and the uncollided component, T_u .

Relations Between Reflection and Transmission and Other Variables Commonly Used in Neutron Transport Theory

The neutron angular distribution function $\psi(\vec{\pi}, \vec{n})$ of Davison and Sykes [24] has a component for each incident and exit particle state and is denoted by $PSI(SE_{1,m}; SI_{j,k})$. The PSI function for the one-dimensional, monoenergetic case is the same as the intensity $I(\tau, \mu, \phi)$ of Chandrasekhar [2].

A systematic nomenclature is used in which $PSIRD$ represents the PSI function based on the diffusely reflected neutrons at the face of the slab on which source neutrons are incident in state $SI_{j,k}$, $PSITD$ represents the PSI function based on the diffuse transmission at the exit face of the slab, and $PSITT$ is based on the total transmission. The PSI functions are obtained by dividing the reflection or transmission by four times the direction cosine of the exit state, i.e.,

$$PSIRD(SE_{1,m}; SI_{j,k}) = \frac{R(SE_{1,m} + NS; SI_{j,k})}{4 MU_1} \quad (2)$$

$$PSITD(SE_{1,m}; SI_{j,k}) = \frac{T(SE_{1,m}; SI_{j,k})}{4 MU_1} \quad (3)$$

$$PSITT(SE_{1,m}; SI_{j,k}) = \frac{T_t(SE_{1,m}; SI_{j,k})}{4 MU_1} \quad (4)$$

where the addition of NS to the exit state index in (2) signifies that the exit direction cosine is the positive (see Chapter III for further details on the state indexing scheme).

Note that PSIRD is the same as the reflection function tabulated by Bellman, Kalaba, and Prestrud [13] for the mono-energetic case with isotropic in the laboratory coordinate system scattering.

The neutron vector net current $j(\vec{r})$ of Davison and Sykes [24] has components for each incident neutron state and each exit energy group, the exit angular dependence having been removed by integration. At this point, the assumption is made that the source has an isotropic angular distribution and the incident angular dependence is also removed by integration. With this assumption, the vector current has a component $J_{m,k}$ for each incident and exit energy group. The diffuse and total vector currents at the incident (0) face and at the face at distance x from the source face are

$$JOD_{m,k} = \frac{1}{4} \sum_{j=1}^{NMUREG} WMU_j \sum_{l=1}^{NMUREG} WMU_l R(SE_{l,m} + NS; SI_{j,k}) \quad (5)$$

$$JOT_{m,k} = JOD_{m,k} + \frac{0.25}{WE_k} \phi_{m,k} \quad (6)$$

$$JXD_{m,k} = \frac{1}{4} \sum_{j=1}^{NMUREG} WMU_j \sum_{l=1}^{NMUREG} WMU_l T(SE_{l,m}; SI_{j,k}) \quad (7)$$

$$JXT_{m,k} = \frac{1}{4} \sum_{j=1}^{NMUREG} WMU_j \sum_{l=1}^{NMUREG} WMU_l T_t(SE_{l,m}; SI_{j,k}) \quad (8)$$

where the minus sign in (6) comes about because the diffuse reflected current is directed in the minus x direction and $\delta_{m,k}$ is the Kronecker delta.

The scalar flux $\rho(\vec{r})$ of Davison and Sykes [24] has a component for each incident particle state and each exit energy range. With the assumption of an isotropic source and an integration over the incident source, the scalar flux has a component $RHO_{m,k}$ for each incident exit and energy group. The diffuse and total scalar fluxes at the incident (0) face and at the face at distance x from the source face are

$$RHOOD_{m,k} = \frac{1}{4} \sum_{j=1}^{NMUREG} WMU_j \sum_{l=1}^{NMUREG} WMU_l \frac{R(SE_{l,m} + NS; SI_{j,k})}{MU_l} \quad (9)$$

$$RHOOT_{m,k} = RHOOD_{m,k} + \frac{0.5}{WE_k} \delta_{m,k} \quad (10)$$

$$RHOXD_{m,k} = \frac{1}{4} \sum_{j=1}^{NMUREG} WMU_j \sum_{l=1}^{NMUREG} WMU_l \frac{T(SE_{l,m}; SI_{j,k})}{MU_l} \quad (11)$$

$$RHOXT_{m,k} = \frac{1}{4} \sum_{j=1}^{NMUREG} WMU_j \sum_{l=1}^{NMUREG} WMU_l \frac{T_t(SE_{l,m}; SI_{j,k})}{MU_l} \quad (12)$$

The scalar flux due to a unit isotropic fission source has a component for each exit energy group and is given by

$$FLUX_1 = \sum_{k=1}^{NEREG} FISS_k RHOXT_{m,k} \quad (13)$$

where $FISS_k$ is the fraction of fission spectrum neutrons emitted in energy group k.

The dose at the exit face of the slab due to a unit isotropic fission source is

$$\text{DOSE} = \sum_{l=1}^{\text{NEREG}} \text{WE}_l \text{RFFCD}_l \text{FLUX}_l \quad (14)$$

where RFFCD_l is the flux-to-dose conversion factor. The usual units for RFFCD_l are millirad/hr per neutron/cm²-sec [25].

Relation Between Point and Plane Sources

The moments method results tabulated by Krumbein [26] are mostly for a point source geometry whereas the invariant imbedding method results are for a plane source geometry.

In an infinite, homogeneous medium, the following relations are valid [27]

$$D_{\text{plane}}(z) = 2\pi \int_z^{\infty} D_{\text{point}}(R) R \, dR \quad (15)$$

$$D_{\text{plane}}(z) = -(1/2\pi z) \frac{d}{dz} D_{\text{plane}}(z) \quad (16)$$

where $D(z)$ is the dose at distance z from a unit point or plane source.

Equation (15) may be used to convert the moments method results to plane geometry. It should be noted that the application of (16) to the invariant imbedding results is not strictly valid because the invariant imbedding results are for a finite medium and include the effects of the boundaries.

This difference between an infinite and a finite medium makes an exact comparison between the moments method and the invariant imbedding method results impossible, however the difference should be small for a very thick slab.

APPENDIX C
COMPUTER PROGRAM FOR THE SOLUTION OF THE
REFLECTION AND TRANSMISSION EQUATIONS

The computer program for the solution of the plane geometry reflection and transmission equations given in Chapter III has been named program STAR where STAR stands for Slab Transmission and Reflection. Program Star is written in the MAD programming language [30] and is suitable for use with either the time sharing or normal FMS batch processing systems at the M. I. T. computation center.

All data is read using the simplified "read data" statement which reads data in the form $A = 1.$, $B = 2.$, ... until the symbol * is encountered. A comment is printed before each use of the "read data" statement indicating what information is required. The data required by any single "read data" statement may be arranged in any order (or omitted if no change from previous data is desired) except that arrays must follow the MAD convention of varying the last subscript most rapidly and terminating * must always be present even if no data is to be read in.

Most of the output is printed out using the "print results" statement.

The program uses the first-order exponential approximation given in Chapter III, with the automatic step size adjustment, if desired, to control the error buildup and to allow easy introduction of materials of widely varying properties.

The program will handle up to 64 particle states in its present form, i.e., the product of the number of energy groups and the number of angular groups must be 32 or less (each angular group represents two particle states with direction cosines of opposite sign). Up to 256 different regions in a heterogeneous array of slabs may be used.

Program STAR is divided into a main program and five subprograms. The required and optional input is given

in the remarks in the first portion of the input subprogram.

An abbreviated description in words of the main program of Program STAR is given (the figures in parentheses are statement numbers) followed by flow diagrams for the subprograms.

A listing of the main and subprograms and sample problem input follow. The sample problem was used for the rod model problems and illustrates the ability to read in new parameters controlling the spacing of the printed points, etc., by using the heterogeneous feature and reading in the new parameters along with the same or different cross sections when desired.

Main Program Description

Read, print, and process input data; initialize variables
(QQ0)

Compute right-hand-sides of R and T differential equations
(QQ10)

Exchange variables

Check step sizes (QQ15)

Compute new R and T values (QQ25)

Compute right-hand-sides of R and T differential equations

Compute estimated stepwise errors

Whenever step size is fixed (QQ80)

- 1) increment variables (QQ110)
- 2) print output, if desired (QQ120)
- 3) exchange variables
- 4) check end of problem conditions and reflection
equation cutoff criterion
- 5) transfer back to statement QQ25

Whenever only transmission was calculated:

- 1) increment variables (QQ100)
- 2) calculate new step size if reflection has been set
to a constant value and transmission step size has
not reached its maximum allowable value
- 3) print output, if desired
- 4) exchange variables

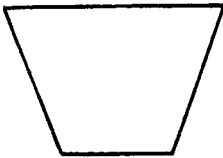
- 5) check end of problem conditions and reflection equation cutoff criterion
- 6) check index for next reflection computation (when transmission step size is smaller than reflection step size)
- 7) whenever reflection has been set to a constant value:
 - a) set transmission only control parameter
 - b) check step size
- 8) transfer back to statement QQ25

When both reflection and transmission were calculated and the step size is not fixed:

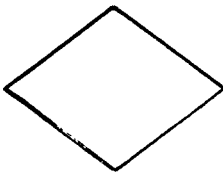
- 1) compute new step size based on the error criterion and estimated stepwise error
- 2) whenever estimated error is over twice as large as the error criterion
 - a) increment index which will cause problem to terminate when index reaches 20
 - b) print step sizes, estimated errors, etc.
 - c) check index and terminate problem if index exceeds 20
 - d) change to new step sizes and return to statement QQ15
- 3) increment variables
- 4) print output, if desired
- 5) check end of problem conditions and reflection equation cutoff criterion
- 6) exchange variables
- 7) check step sizes
- 8) when the error criterion is less than equal to zero
 - a) fix the step size at the smaller of the new reflection and transmission step sizes
 - b) set for transmission only calculation when the reflection equation cutoff condition has been reached
- 9) change to new step sizes allowing the transmission step size to be an integral subdivision of the reflection step size if called for
- 10) set index which counts transmission only computations back to zero
- 11) whenever the transmission step size is less than the reflection step size, set transmission only control parameter
- 12) whenever reflection equation cutoff condition has been reached, set transmission only control parameter
- 13) return to statement QQ25.

**PROCESSING**

A group of program instructions which perform a processing function of the program.

**INPUT/OUTPUT**

Any function of an input/output device.

**DECISION**

The decision function used to document point in the program where a branch to alternate paths is possible.

**PREDEFINED PROCESS**

A group of operations not detailed in the particular set of flow charts.

**TERMINAL**

The beginning, end, or a point of interruption in a program.

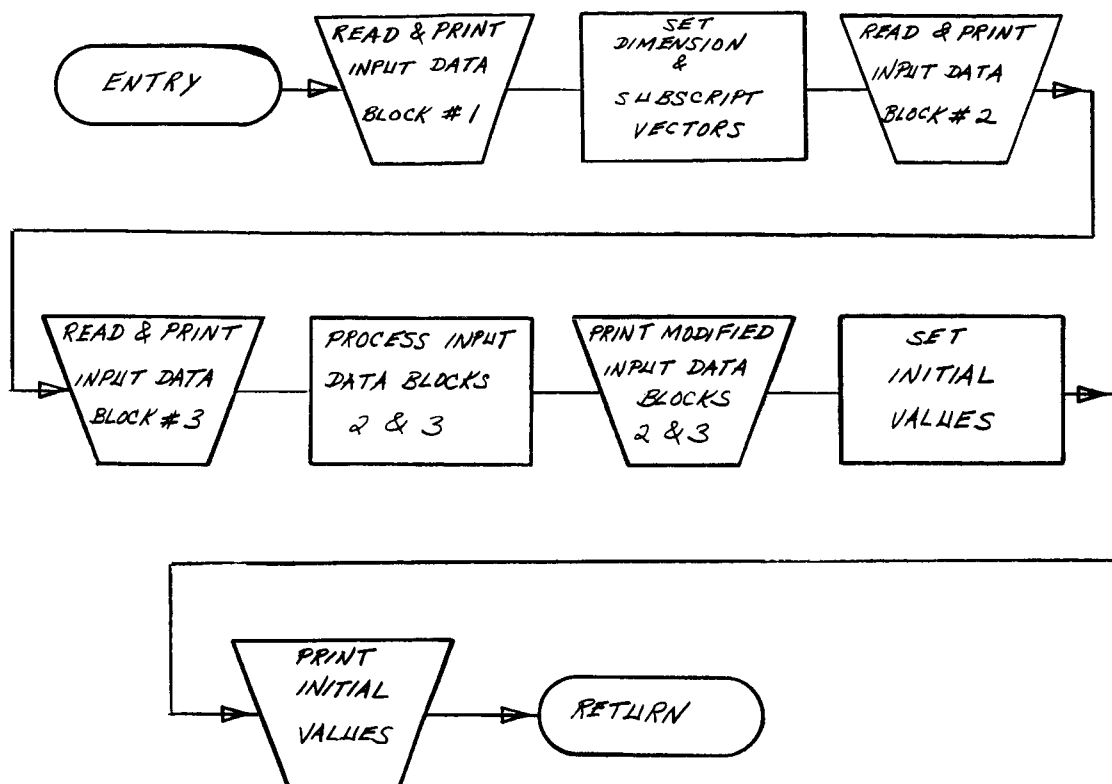
**CONNECTOR**

An entry from, or an exit to, another part of the program flowchart.

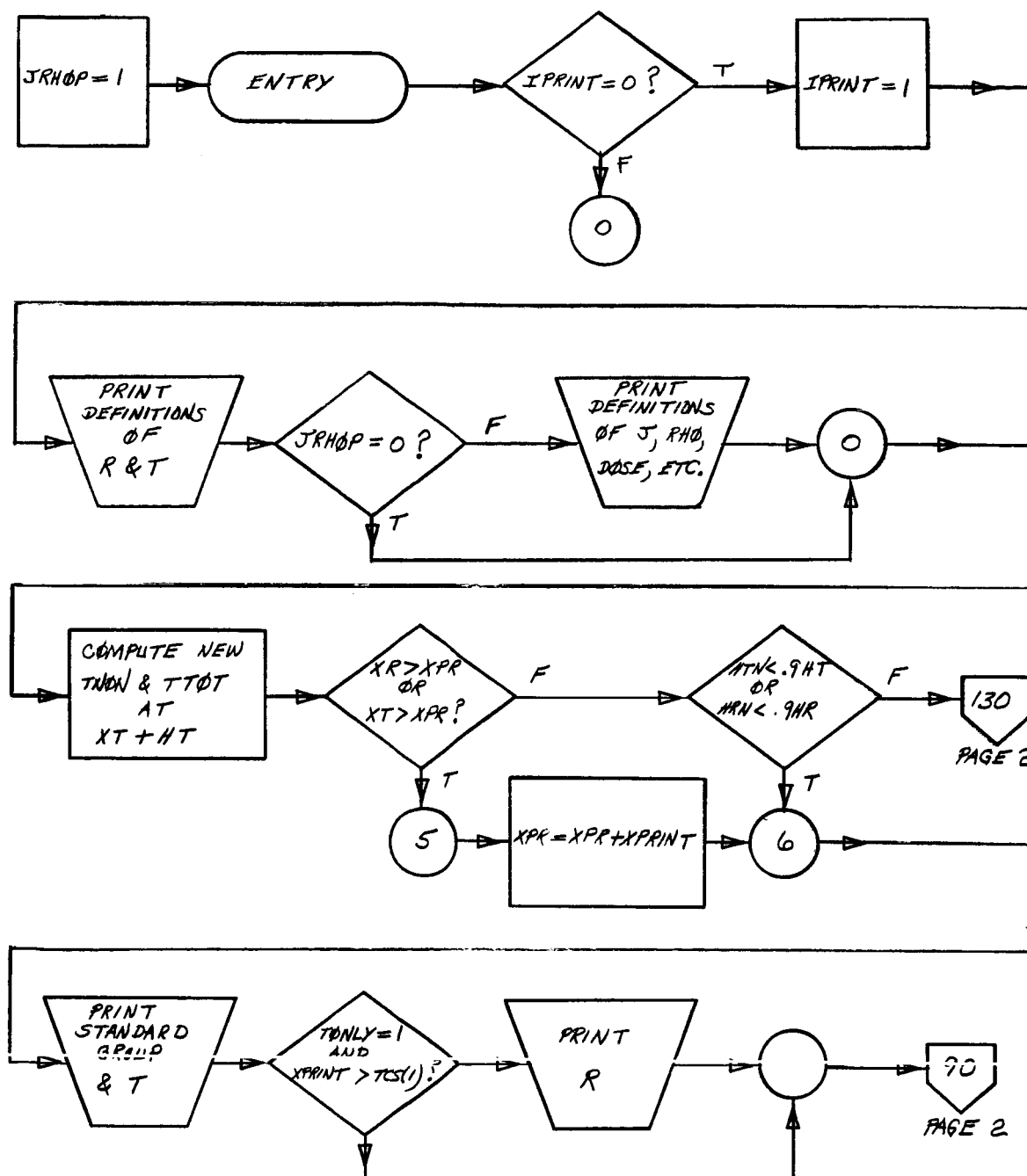
**OFFPAGE CONNECTOR**

A connector used instead of the connector symbol to designate entry to or exit from a page.

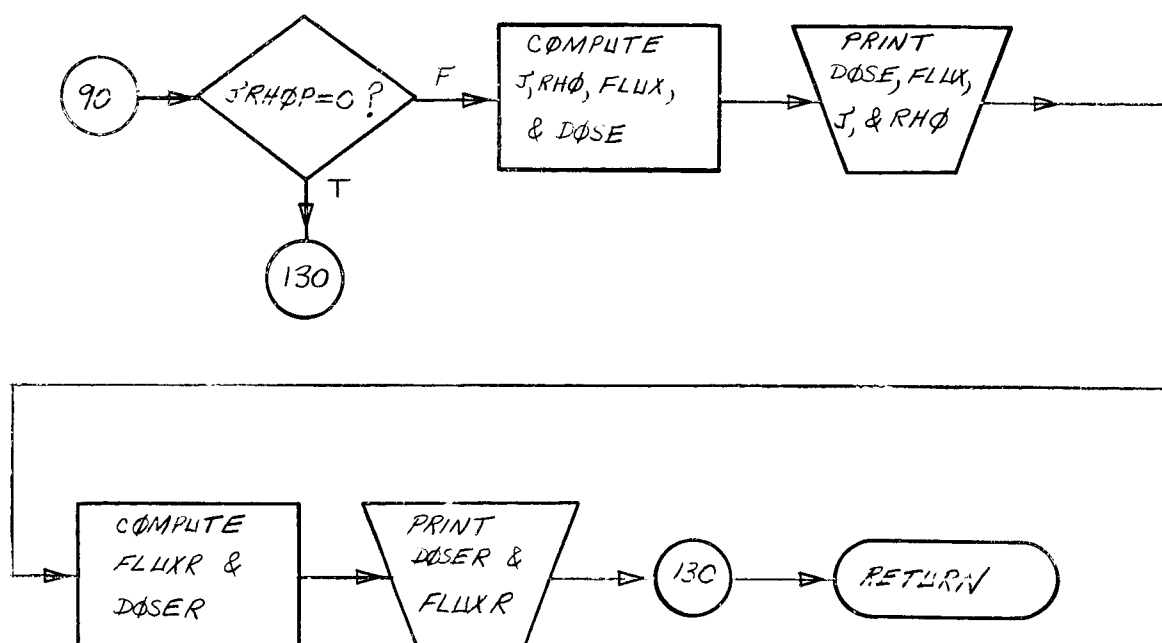
PROGRAM FLOWCHART SYMBOLS



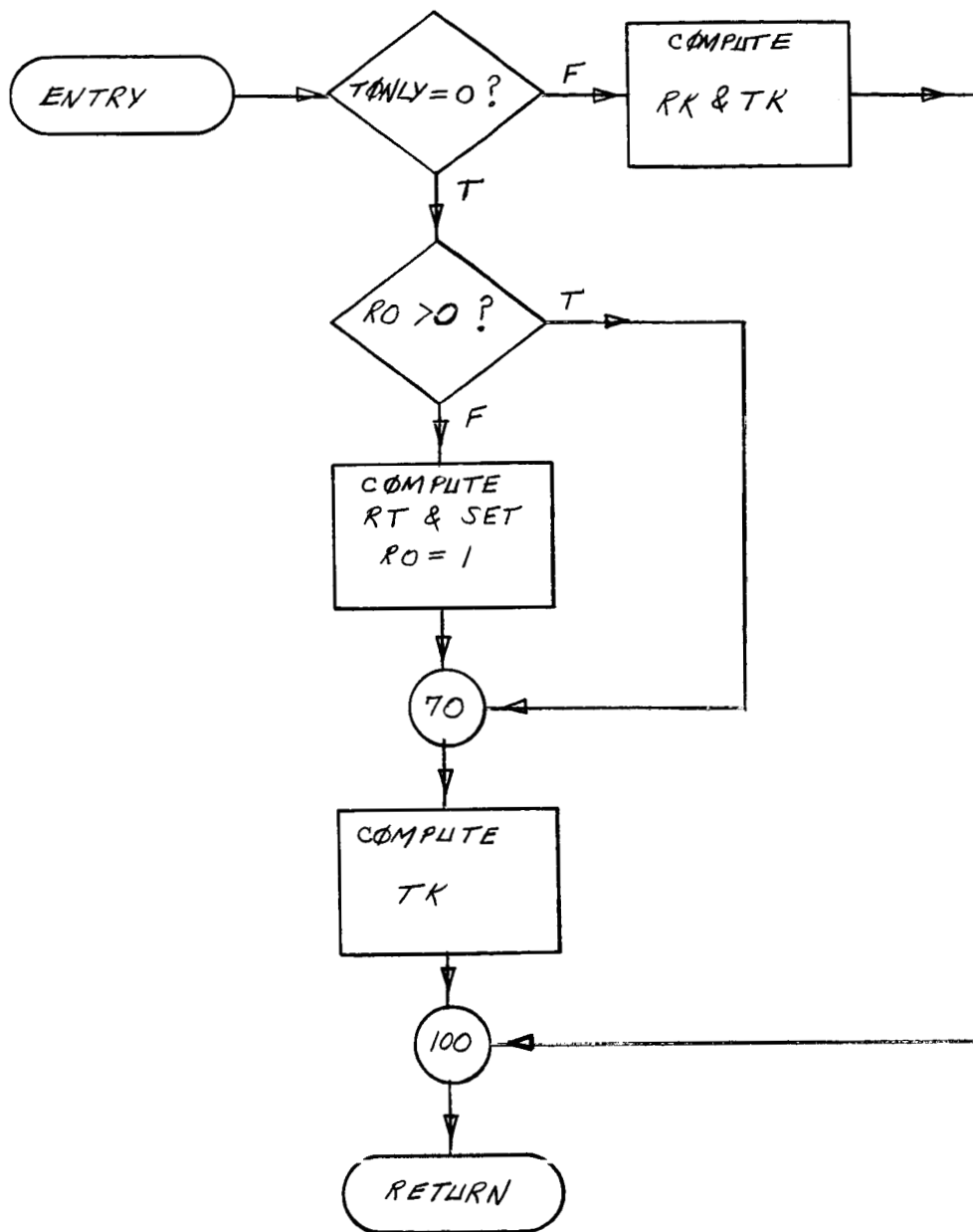
FLOW DIAGRAM FOR INPUT SUBPROGRAM (PAGE 1 OF 1)



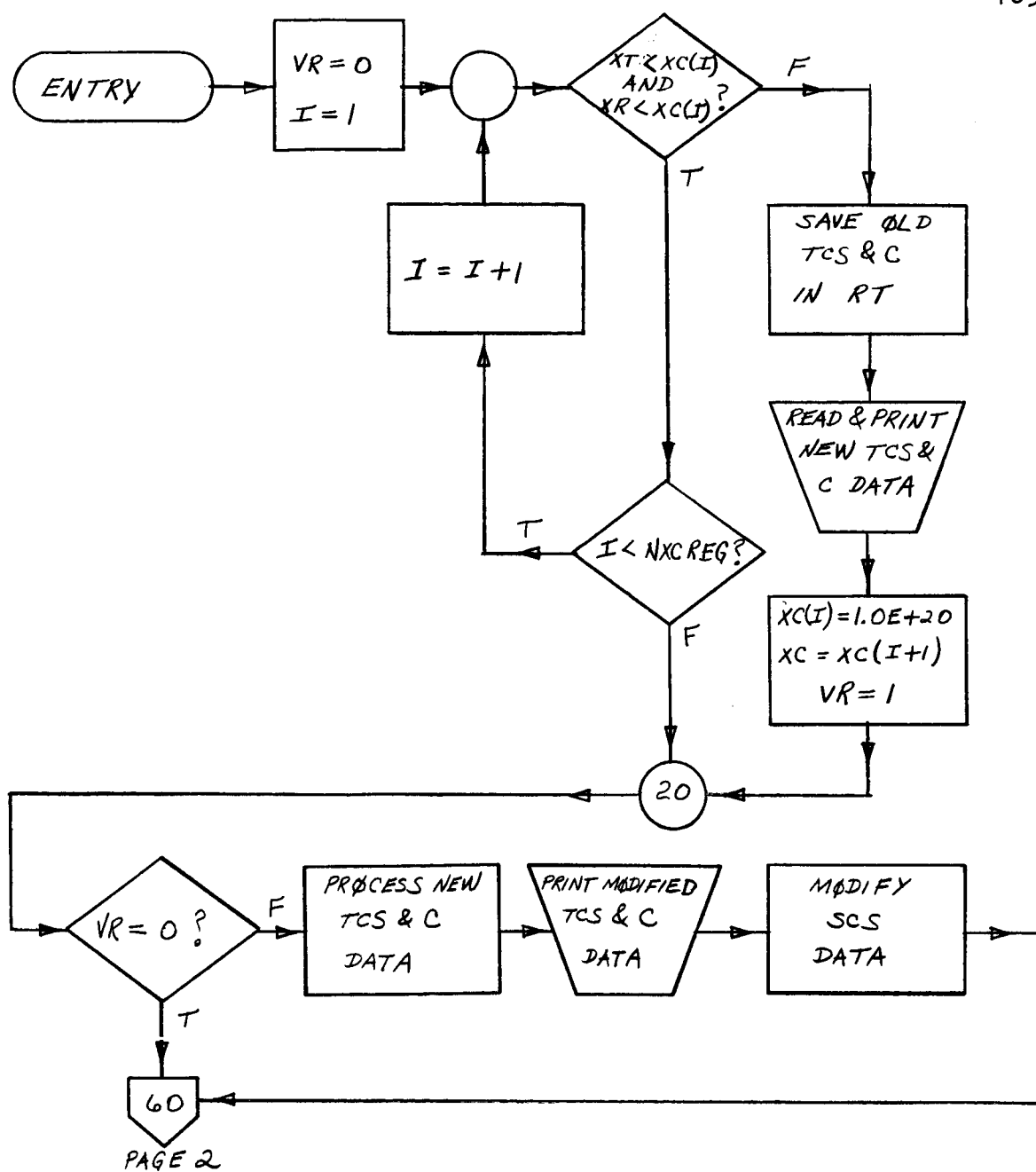
FLOW DIAGRAM FOR OUTPUT SUBPROGRAM (PAGE 1 OF 2)



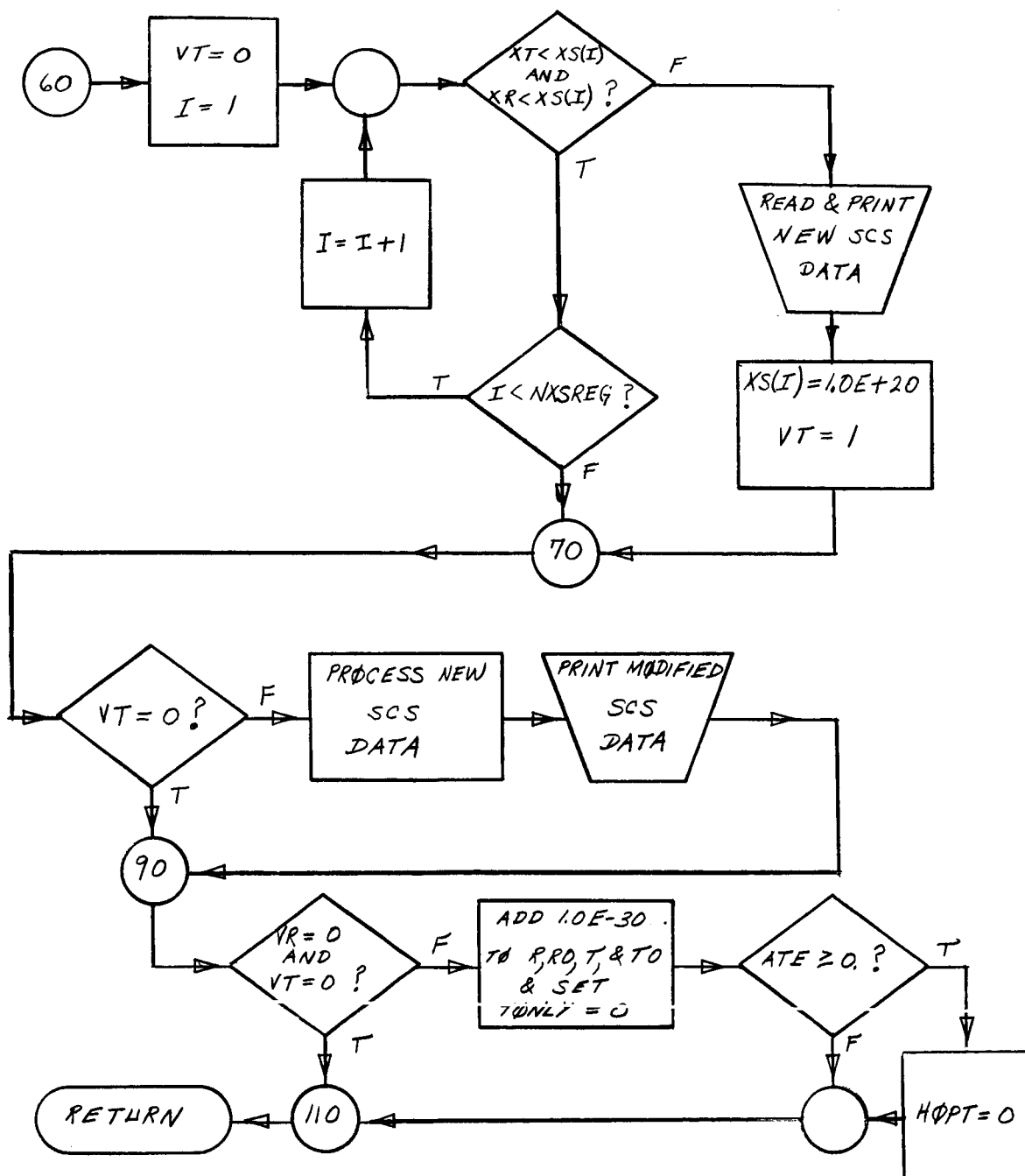
FLOW DIAGRAM FOR OUTPUT SUBPROGRAM (PAGE 2 OF 2)



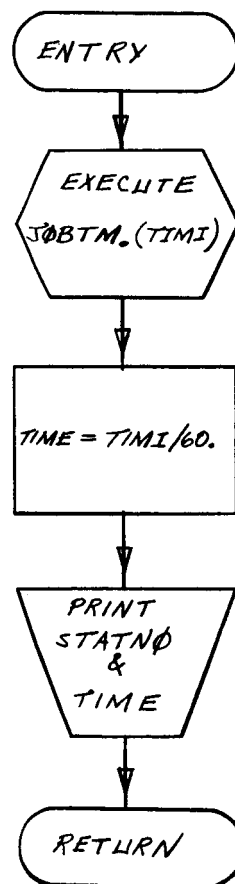
FLOW DIAGRAM FOR RHS SUBPROGRAM (PAGE 1 OF 1)



FLOW DIAGRAM FOR DATA SUBPROGRAM (PAGE 1 OF 2)



FLOW DIAGRAM FOR DATA SUBPROGRAM (PAGE 2 OF 2)



FLOW DIAGRAM FOR TIM SUBPROGRAM (PAGE 1 OF 1)

{ The listings of Program STAR and the sample problem
occupy pages 112 through 137 of the original copies of
this thesis filed with the Nuclear Engineering Department,
The Massachusetts Institute of Technology, Cambridge,
Massachusetts. }

APPENDIX D

COMPUTER PROGRAM FOR THE PREPARATION OF INPUT DATA

The cross section data preparation program is written in the MAD programming language [30] and is suitable for use with either the time sharing system or normal FMS batch processing at the M. I. T. computation center.

All data is read using the simplified "read data" statement which reads data in the form $A=1., B=2., C=3., \dots$ until the symbol * is encountered. A comment is printed before each use of the "read data" statement indicating what information is required. The data required by any single "read data" statement may be arranged in any order (or omitted if no change from previous data is desired) except that arrays must follow the MAD convention of varying the last subscript most rapidly and a terminating * must be present even if no data is to be read in.

All data is printed out using the "print results" statement.

The program is dimensioned to accept cross sections for a maximum of 5 nuclides tabulated at 100 energy points or any other combination of nuclides and energies requiring 500 or less storage locations.

The following data is punched out in a suitable format to be read with the "read data" statement in program STAR:

1. NEREG = number of energy groups (maximum of 16)
2. E(1)...E(NEREG) = energy assigned to each energy group
3. W(1)...WE(NEREG) = width of each energy group
4. FISS(1)...FISS(NEREG) = fraction of fission spectrum in each energy group
5. NMUREG = number of direction cosine groups (maximum of 16) (NS = NEREG*NMUREG must be 32 or less)

6. MU(1)...MU(NMUREG) = direction cosine assigned to each direction cosine group
7. WMU(1)...WMU(NMUREG) = width of each direction cosine group
8. TCS(1)...TCS(NEREG) = total macroscopic cross section for each energy group
9. C(1)...C(NEREG) = mean number of secondaries per collision for each energy group
10. SCS(1,1)...SOS(NS,2*NS) = state-to-state transfer probability matrix.

A listing of the program, sample problem input, and sample problem output follows. The sample problem was used for the preparation of 4 energy group, 2 angular group cross sections for polyethylene based on carbon and hydrogen cross sections tabulated at 9 energy points in the energy interval from .33 Mev to 18.017 Mev.

{ The listings of the cross section data preparation program and sample problem input and output occupy pages 140 through 167 of the original copies of this thesis filed with the Nuclear Engineering Department, The Massachusetts Institute of Technology, Cambridge, Massachusetts. }

REFERENCES

A. GENERAL REFERENCES

1. Chandrasekhar, S., "Radiative Transfer," Dover Publ., Inc., New York, 1960.

This is a reprint of Chandrasekhar's excellent 1950 book summarizing his development of the invariant imbedding method under the name "principles of invariance."

2. Bellman, R., R. Kalaba, and G. M. Wing, "Invariant Imbedding and Mathematical Physics. I Particle Processes," J. Math. Phy. 1, 280 (1960).

A good summary paper with many references to other work.

3. Beissner, R. E., "The Application of Invariant Imbedding to Shielding Problems," Report NARF-61-41T, General Dynamics, Fort Worth, March 9, 1962.

Good exposition with monoenergetic results.

4. Wing, G. M., "An Introduction to Transport Theory," John Wiley and Sons, Inc., New York, 1962.

Compares invariant imbedding and Boltzmann approaches to a number of problems.

5. Bellman, R. E., R. E. Kalaba, and M. C. Prestrud, "Invariant Imbedding & Radiative Transfer in Slabs of Finite Thickness," American Elsevier Publ. Co., Inc., New York, 1963.

Presents detailed numerical solution of the monoenergetic reflection equation in isotropic scatter case.

B. REFERENCES CITED IN TEXT

1. Ambarzumian, V. A., cited on p. 104 of Ref. 1 of the previous section.
2. See Ref. 1 of the previous section.
3. Bellman, R., R. Kalaba, and G. M. Wing, "On the Principle of Invariant Imbedding and Neutron Transport Theory-I: One Dimensional Case," J. Math. & Mech. 7, 149 (1958).
4. See Ref. 3 of the previous section.
5. See Ref. 2 of the previous section.
6. Beissner, R. E., "An Analysis of Fast-Neutron Energy-Angle Distributions," Report NARF-63-186, General Dynamics, Fort Worth, August 15, 1963.
7. Hildebrand, F. B., "Advanced Calculus for Applications," Prentice Hall, Inc., Englewood Cliffs, New Jersey, 1964.
8. See Ref. 4 of the previous section.
9. Hildebrand, F. B., "Introduction to Numerical Analysis," McGraw-Hill Book Co., Inc., New York, 1956.
10. Ralston, A. and H. S. Wilf (eds.), "Mathematical Methods for Digital Computers," John Wiley & Sons, Inc., New York, 1964.
11. Hansen, K. F., B. V. Koen, and W. W. Little, Jr. "Stable Numerical Solutions of the Reactor Kinetics Equations," Nucl. Sci. Eng. 22, 51 (1965).
12. Certaine, J., "The Solution of Ordinary Differential Equations with Large Time Constants," pp. 128-132 of Ref. 10 above.
13. See Ref. 5 of the previous section.
14. Ashley, R. L. and W. E. Kreger (eds.), "Neutron Attenuation in Optically Thick Shields," Report ANS-SD-1, American Nuclear Society, Hinsdale, Illinois, 1964.
15. Allen, F. J., A. T. Futterer, and W. P. Wright, "Neutron Transmission Versus Thicknesses for Some Common

- Materials," Report BRL-1174, Ballistic Research Laboratories, Aberdeen Proving Ground, Maryland, 1962.
16. Mayers, D. F., "Calculation of Chandrasekhar's X- and Y-Functions for Isotropic Scattering," Monthly Notices Roy. Astr. Soc. 123, 471 (1962).
 17. Aronson, R., J. Certaine, H. Goldstein, and S. Preiser, "Penetration of Neutrons From a Point Isotropic Fission Source in Water," Report NYO-6267, Nuclear Development Associates, Inc., White Plains, New York, 1954.
 18. Goldstein, H., "Neutron Cross Sections for Neutron Attenuation Problems Proposed by the ANS Shielding Division," Contribution 63-31-1 of the Division of Nuclear Science and Engineering, Columbia University, New York, 1963.
 19. Gast, R., "On the Equivalence of the Spherical Harmonics Method and the Discrete Ordinate Method Using Gauss Quadrature for the Boltzmann Equation," Report WAPD-TM-118, Westinghouse Electric Corp., Bettis Plant, Pittsburgh, 1958.
 20. Chandrasekhar, S., "On the Diffuse Reflection of a Pencil of Radiation by a Plane-Parallel Atmosphere," Proc. Natl. Acad. Sci. (U. S. A.) 44, 933 (1958).
 21. Bailey, P. B. and G. M. Wing, "A Correction to Some Invariant Imbedding Equations of Transport Theory Obtained by "Particle Counting," J. Math. Anal. & App. 8, 170 (1964).
 22. Lowan, Arnold R., Norman Davids, and Arthur Levenson, "Tables of the Zeros of the Legendre Polynomials of Order 1-16 and the Weight Coefficients for Gauss's Mechanical Quadrature Formula," Bull. Am. Math. Soc. 48, pp. 739-743 (1942).
 23. Weinberg, A. M. and E. P. Wigner, "The Physical Theory of Neutron Chain Reactors," University of Chicago Press, 1958, pp. 279-285.

24. Davison, B. and J. B. Sykes, "Neutron Transport Theory," Oxford University Press, London(1957), pp. 41-42 & p. 256.
25. Goldstein, H., "Fundamental Aspects of Reactor Shielding," Addison-Wesley Publishing Co., Inc., Reading, Mass. (1959), p. 20.
26. Krumbein, A. D., "Summary of NDA Unclassified Results of Moments Calculations for the Penetration of Neutrons Through Various Materials," U. S. A. E. C. Report NDA-92-2(Rev.), Nuclear Development Corporation of America, White Plains, New York, August 30, 1957.
27. Blizard, E. P. on p. 130 of the "Reactor Handbook, Volume III Part B Shielding," E. P. Blizard and L. S. Abbot Editors, Interscience Publishers Division of John Wiley & Sons, New York(1962).
28. Yarmush, D., J. Zell, and R. Aronson, "The Transmission Matrix Method for Penetration Problems," Report WADC-TR-59-772, Technical Research Group, Inc., Syossett, New York, Aug. 1960.
29. SHARE Distributions 413 and 827, DP Program Information Department, IBM Corp., White Plains, New York.
30. Arden, B., B. Galler, and R. Graham, "The Michican Algorithm Decoder," The University of Michigan Computing Center, Ann Arbor, Michigan, November 1963.

BIOGRAPHICAL SKETCH

The author was born in Madera, California, in 1931 and attended Elementary and High School in Chowchilla, California. His undergraduate education at the University of California at Berkeley was interrupted by a tour of duty in the U.S. Army from 1951 to 1954 where he was trained as an interpreter in the Russian language. He graduated from the University of California at Berkeley in 1958 with a B.S. in Engineering Physics, and again in 1959 with an M. S. in Nuclear Engineering.

From 1959 to 1962, he worked as a nuclear engineer and shift supervisor for the Aerojet-General Nucleonics Corporation in San Ramon, California, and later in Idaho Falls, Idaho, on the design, construction, and operation of the ML-1 mobile high temperature gas-cooled reactor.

In 1962, he received an AEC Special Fellowship in Nuclear Science and Engineering, and entered M.I.T. to work on a doctorate in Nuclear Engineering.

He married Eleanor Lynn Venstrom of Berkeley, California, in 1958. They have three children, Kristine Annette, age 6½, Duane Alan, age 4½, and Sharon Marie, age 2½.

He received the Richard A Fayram Memorial Award in Nuclear Engineering from the Nuclear Engineering Department of the University of California at Berkeley in 1959 and is a member of Tau Beta Pi, Sigma Xi, and the American Nuclear Society.

The Oak Ridge National Laboratory has published a report (ORNL-3178) based on work by the author and others on shielding problems related to the ML-1 reactor conducted at the Lid Tank Shielding Facility at Oak Ridge. Preliminary results of this thesis research were published in the Trans. Am. Nucl. Soc., 8, 508(1965).